# *Part V*
# *Textile processing and testing*

# 22

# INTRODUCTION

Parts II, III and IV have dealt with fibre breaks in the informative but artificial situation of laboratory studies of single fibres. In Part V we come closer to the reality of fibre utilization by industry and the consumer.

We examine first fibre ends which result from textile processing. Apart from the inherent interest in these breaks, it is important to be able to recognize them as not being a result of wear itself, when they occur in case studies of wear of textile materials. We then consider laboratory tests on textile materials: yarns, fabrics and composites. Sometimes such tests are used as easier ways of studying single-fibre properties, because the test specimens are larger, but more often they are used as a guide to performance of materials in use.

# 23

# PROCESSED AND NATURAL FIBRE ENDS

When the raw material for the textile industry is supplied in the form of baled fibres, each bale will contain at least $10^{10}$ fibre ends, which will have either developed naturally or have been produced during harvesting or shearing of natural fibres or cutting of man-made fibre tow. Another way of converting tow into staple fibres is to break the filaments on a stretch-breaking machine as a first stage of textile processing. All these fibre ends will show up in textile materials.

Cutting of staple fibre gives a distorted and complicated fibre end, **23A(1)–(3)**, which may be a mixture of true cutting and pulling the fibre apart by tension. Stretch-breaking gives a tensile break, **23A(4)**, although in nylon and polyester this will have the mushroom form of a high-speed break. Cotton shows a difference between the natural tip of the fibre, **23A(5)**, and the root, **23A(6)**, in fibres taken from a bale. Cotton fibres damaged by processing may show a more ragged appearance, **23A(7)**, possibly associated with multiple splitting due to bending and twisting.

Apart from accidental and unwanted fibre breakage during textile processing, there is some deliberate formation of fibre ends. For example, the hairiness of a textile fabric may be reduced by singeing, and this leads to the bulbous polyester fibre ends in **23B(1)**. In some very open and hairy fabrics, singeing can cause problems if fibres get melted in two places and break off, as shown in the light microscope view in **23B(2)**. Other examples of singeing are in **29A(1)** and **34D(1)**.

The contrary situation is found in fastener fabrics, like Velcro, where fibre ends sticking out of the fabric have a positive role to play. The fibres are fairly thick monofilaments, and the form of the ends depends on the nature of the fibre and how it has been cut, **23B(3a,b)**. It is necessary to have a loop or a mushroom end, in order to cause the fastening to occur. The mushroom end probably results from cutting with a hot wire between two layers of a double fabric linked by the monofilaments, but the loops are formed by cutting a loop pile.

Finally there are situations in which fibres are cut in order to produce a pile fabric. Velvet can be woven or knitted as a double fabric, and then cut between the two layers by a sharp knife, to give fibre ends, **23B(4)**, similar to fibres cut with a razor. Another example in a cotton cord fabric is shown in **28F(3)**. In cut pile carpets the loops which are formed in tufting or weaving are more crudely cut, and the ends look more like blunter knife cuts, **23B(5),(6)**. Other examples are in **33F(1),(2)**.

---

Fibres are subject to damage as a result of the severe forces that can be imposed on them during textile processing. One example consists of the actions in the early stages of wool processing, which are described below. However the 'damage' is not always harmful; it can be at least partly beneficial if not wholly necessary. In this chapter both categories are illustrated.

Davis (1989) describes the way in which multiple carding increases the dyeability of polyester fibres. The staining technique for transmission electron microscopy, which was described in Chapter 1, provides pictures to explain the reasons for this. A low magnification view, **23C(1)**, of a trilobal polyester fibre, which had been subject to three laboratory cardings, shows three kinds of damage: 'first, the surface is highly distorted; second, a large number of cracks are observed in the fibers; third, much of the lobe area appears to absorb substantially more stain than would normally be expected.' Higher magnification, **23C(2)**, shows that 'the internal boundary structure has opened up in the vicinity of the cracks and in the dark stained regions', and therefore 'would be expected to diffuse and absorb dye rapidly, just as it does with the stain'.

The next two pictures show deliberate rupture of fibres in the stretch-breaking of a continuous filament acrylic tow into staple fibres. **23C(3)** has the characteristic granular tensile fracture of acrylic fibres, as seen, for example, in **8B(2)**, but there is splitting in **23C(4)**, which is more like **8C(2b)**.

As an example of controlled attack, **23C(5),(6)** show the effects of treating polyester fibres with caustic soda, so as to reduce their diameter and change their surface character. This can give an enhanced appearance and feel to fabrics.

In order to make paper, wood-pulp fibres must be caused to fibrillate by beating in the wet state. **23D(1),(2)**, from Hamad and Provan (1995), shows how the outer layers of the fibre are removed and inner layers break up into fibrils.

In many other processes, damage is undesirable and should be avoided as far as possible. Studies by Greenwood and Cork (1984) show the intense fibrillation which results from abrasion during the weaving of Kevlar aramid fabrics, **23D(3),(4)**. The failure of filaments causes a substantial reduction in yarn strength. There are fibrils in unwoven yarn, **23D(5),(6)**, but to a much smaller extent.

The appearance of fabrics of the new lyocell fibre, Tencel from Courtaulds, at various stages of processing is shown in **23E** and **23F**. The fibre, which consists of cellulose spun from an organic solvent, fibrillates easily. Properly controlled, this can give a very attractive hand to fabrics. As woven, **23E(1),(2)**, the fibres appear circular with hardly any fibrillation. They are even cleaner after singeing and desizing, **23E(3),(4)**. However, after steam-tumbling, **23E(5),(6)**, there is extensive fibrillation. Other stages of processing are shown in **23F(1)–(4)**. Finally, enzyme treatment, **23F(5),(6)**, enhances the appeal of the fabrics.

## WOOL FIBRE RUPTURE AND MICRODAMAGE IN OPENING PROCESSES

**by Nigel Johnson and Ali Akbar Gharehaghaji**

Fibres are mechanically damaged during their conversion from raw fibre to finished product. Opening processes, which separate clumps of fibres into smaller clumps and even into individual fibres, can be particularly damaging, often evidenced as a significant shortening of the mean fibre length. In loose fibre opening processes, such as those found in the blowroom and carding, opening elements (e.g., pins or sawtooth wire mounted on rollers) tear through fibre clumps in order to straighten and disentangle them. Similarly, sliver opening involves pin or wire opening elements passing through more aligned assemblies of fibres; specially severe is the sliver opening necessary to create the fibre flow for open-end spinning.

Wool fibres are particularly prone to damage in opening processes, often getting broken because of their relatively low tenacity. Their crimp and long length make them difficult to separate into individual fibres, while debris from removed surface scales leads to rotor deposits in conventional rotor spinning.

A series of investigations has attempted to uncover the forms of damage that occur in opening processes. These investigations were conducted with pristine fibres to ensure that the observed damage did not occur in some earlier process. Even with unprocessed wool, the fibre tips are weathered (degraded by sunlight) and the root ends severed by the shearer s cutting blades, so experimental fibres are prepared by cutting off both ends with scissors. Good fibre uniformity can be achieved by selecting fibres from hand-fed sheep kept indoors. An original fibre end, with the weathered tip removed by a scissor cut, is shown in **23G(1)**.

Following preliminary work by Young and Johnson (1988, 1990), Yan (1991) studied the fracture morphology of ruptured fibre ends. Using the opening unit of an Investa BDA12 long staple rotor spinner, he explored the effect of opening roller speed. The BD A12 opening rollers were unusual in that they consisted of widely-spaced rows of sawtooth wire set across the roller surface, parallel to the axis. At slow speeds of both opening roller and feed roller, the wire elements travelling at 1000 m/min contact the fibres relatively gently so that no fibres were actually ruptured, but the high number of contacts caused wear. Scale edges were broken and removed and the fibre end was worn down and rounded, **23G(2)**. At a slightly higher element speed of 1100 m/min, there was still no fibre breakage, but with a much faster feed speed (giving fewer pin contacts on the fibre) there was much less wear of the fibre end, although scale lifting was still seen and fibre splitting was sometimes observed, **23G(3)**.

At substantially higher speeds of the opening element (1860 m/min) many of the fibres were broken. The new ends created by this breakage, but still held by the feed rollers, can be struck many further times by the opening elements. These usually developed severe axial splitting, **23G(4)**, or other damage, such as scale lifting, **23G(5)**. Young and Johnson (1988) had observed such fibrillation developing in a section of the fibre prior to rupture, **23G(6)**.

Following Yan's (1991) investigation of damaged fibre ends, Gharehaghaji (1994) searched for the more subtle damage that might be caused to the body of the fibre without actually breaking it. He termed this *microdamage*. He looked for such microdamage in fibres subjected to sliver opening via the opening units of short staple rotor spinners, using pin and sawtooth clothed opening rollers. While both pin and sawtooth elements caused microdamage, that due to the sawtooth was far more severe. It should also be remembered that the fibres could inflict damage on each other as they are pulled out of entanglements or tightly into knots. He found instances of the following features:

- Wearing away of the surface scales, **23H(1)**.
- Transverse cracks, **23H(1)**.
- Transverse cracks which often coincided with the tip edge of the overlapping scale, **23H(2)**.
- Longitudinal cracks, usually together with transverse cracks, **23H(3),(4)**.
- Cracks which were quite large and deep, **23H(5)**.
- Holes, often surprisingly circular and sometimes in clusters giving a honeycomb effect, **23H(6)**. These holes were more prevalent in pin-damaged samples than wire-damaged samples.
- Plastic compressional deformation where the fibre had been partly crushed by the opening element or another fibre, **23H(7)**. The visco-elastic wool fibre might be expected to behave elastically at the impact speeds likely in these experiments, but it appears that the time of contact can be sufficiently long for permanent deformation to occur. This may happen as a fibre is detached from the feed roller and carried forward by the element, or if a fibre is bent sharply around another which is then dragged forward with it.

The interactions between fibres and opening elements are very complex and highly variable in an actual opening process. To get a better understanding of the individual contact process, Gharehaghaji looped fibres around the leading edge of opening elements and pulled the fibre loop against the element at a constant rate of extension in an extensometer; strain rates from 5 to 1000% per minute were investigated. Fibres were extended to two-thirds of their average breaking extension, and immediately released. The element contact regions of those fibres which did not break were then examined. Again, the damage features were more severe when the fibre loop was pulled against the sharp corners of sawtooth wire than against the more gentle rounded shape of the pin.

Seven distinctive features were created in these experiments:

- Longitudinal cracks (axial splits), **23I(1)**, were found only with wire damaged samples. Such cracks are probably caused by the high shear stress associated with the strong variable curvature bending at the square edges of the sawtooth.
- Transverse cracks occurred at the outside of the bend in both wire and pin-damaged samples. In **23I(2)**, some fibre debris lies towards the camera; the compressed region, which contacted the sawtooth edge, is on the left; and a transverse crack can be seen to the right. Transverse cracks became more frequent at higher strain rates.
- Permanent compressive deformation was commonly caused by the sharp corners of the sawtooth wire, **23I(3)–(6)**, but only at the lower rates of strain. At the faster rates, the fibre behaved more elastically and was able to recover from the deformation. In some cases, the concentration of axial and lateral compressive stresses led to platelet buckling.
- Scale lifting, **23I(7)**, was more common at the higher rates of strain, on the outside of the bend.
- Surface wear occurred where the fibre slipped around the element, even though efforts were made to prevent this happening. The sliding action of the sawtooth edge sometimes caused a rippling effect, **23I(8)**.
- Cuts were sometimes created by the sharp edges of the sawtooth wire, **23I(8)**.
- Holes (circular voids) were also created on some of these samples, **23I(9)**.

Some forms of microdamage were also induced at places away from the region of contact with the element. The transverse cracks, including those at the tipline of overlapping scales, scale lifting, longitudinal micro-cracks and holes must have been caused purely by the axial extension.

The effects of opening elements contacting fibres can be examined in even greater detail by using a tensile stage in the scanning electron microscope. The stage allows regions of the fibre to be examined as the fibre is slowly extended, and the progressive changes in the fibre surface can be recorded on video. Using tensile stages, Hepworth *et al* (1969) and Yang *et al* (1988) slowly extended undamaged wool fibres and observed scales lifting from the fibre surface, then transverse microcracks developing, some of which grow into larger cracks. In some instances, necking of the fibre can occur prior to final rupture. The microcracks initiate at critical points, such as natural micro-voids within the fibre and the weak region at the root of overlapping scales where stress concentrates. Another characteristic feature is the craze, a special form of transverse crack which eventually grows rapidly and becomes the rupture site. White lines in the SEM record, see **23J(5)**, are indicative of crazes.

After confirming these observations for simple extension of undamaged fibres, Gharehaghaji extended fibres that had already suffered damage from opening elements. Controlled damage was first inflicted by pressing the edge of the opening elements into a fibre resting on a flat surface. He then observed the damaged region as the fibre was extended slowly in the SEM by a simple tensile stage.

Of course, this does not precisely simulate the action in an opening process, because the damage occurs by slow compression against a flat surface rather than by high speed impact in free space, and the extension is necessarily extremely slow so that changes can be observed and recorded. Nonetheless, it does simulate the mechanical behaviour of a damaged fibre under tensile load in a subsequent process. Very interesting phenomena have been observed which give insights into the forms of microdamage which can weaken the fibre and lead to eventual tensile failure.

**23J(1)** shows an extended fibre which was previously cut by a sawtooth element being pressed into it. As the bulk of the fibre was uniformly strained, the two faces of the cut separated, leading to a shear stress which formed a longitudinal split, initiated at the base of the cut and running in both directions. With further extension, one of these longitudinal splits developed a transverse component, so that the crack propagated at an angle across the fibre, leading to rupture and leaving a tapered ruptured end, similar to that shown in **23J(3)**. Pushing the sawtooth element deeper into the fibre induced permanent deformation, sometimes accompanied by a cut at the sharp edge, **23J(2)**. When this fibre was stretched, an angled longitudinal split developed from the base of the cut and propagated down through the deformed region, leading to rupture, **23J(3)**. Because the deformed region was so much weaker than the fibre above the cut, the longitudinal crack did not propagate into this undamaged side.

The rounded surface of a pin causes much less dramatic damage and in most cases, it is not possible to see any damage on the surface of the compressed fibre before it is stretched. As it is stretched, features similar to those seen in the stretching of undamaged fibre are apparent (lifted scales and transverse cracks), except that they arise preferentially at the damaged site. This is probably because the area is weak and so takes more of the strain energy. In **23J(4)**, a wide crack has opened, allowing a clear view of the stretched interior of the fibre, which has the appearance of an aligned fibrillar material. Some charging is evident on this exposed interior surface because it is not coated. At the left side of this crack and in line with its centre, a new craze (seen as a faint, thin white-lipped crack) can be seen developing, **23J(5)**. This craze grew rapidly and was the site of final rupture.

The effects of the sharp cutting edge of the sawtooth wire were simulated in a more controlled fashion using a sharp blade, pressed into the fibre at a 60° angle to the fibre axis. When such blade-damaged fibres were slowly stretched, a series of transverse crazes developed, **23J(6)**; one of these eventually became dominant, growing into a larger crack which finally burst rapidly through the fibre and ruptured it.

In a second series of dynamic SEM experiments, the tensile stage was used to pull loops of undamaged fibres against opening elements mounted inside the SEM, **23J(7)**. A key difference between these experiments and the previous ones is that the compressive effects are created by the fibre tension, so that the fibre tension may initiate failure before any severe crushing or compressive effects have been induced. In fact, as has already been noted by others, the majority of the fibres pulled around a round pin broke at weak places (natural flaws?) away from the pin contact area. The sharp edges of the sawtooth wire have a more

**Table 23.1** — Experimental materials and threads

a) Experimental materials

| Substrate | Construction | Mass, g/m$^2$ | Fibre content, % |
|---|---|---|---|
| Knitted wool | 1 × 1 knitted rib<br>7.0 wales/cm<br>10.0 courses/cm | 408.2 | 100 wool |
| Knitted cotton | Knitted interlock<br>12.5 wales/cm<br>14.5 courses/cm | 170.4 | 100 cotton |
| Woven wool | Woven twill<br>Z 2/1steps<br>22 warp yarns/cm<br>22 weft yarns/cm | 318.5 | 67.4 wool<br>31.8 acrylic<br>0.8 elastomer |

b) Threads

| Thread | Construction | Turns/m | Breaking load, N | Breaking extension, % | Count, tex | Diameter, mm |
|---|---|---|---|---|---|---|
| Mercerised cotton | 3-fold yarn | 636 | 12.6 | 5.61 | R49/3 | 0.21 |
| Spun polyester | 3-fold yarn<br>Folding Z twist<br>singles S twist | 733 | 11.9 | 18.29 | R34/3 | 0.18 |
| Continuous filament polyester | 3-fold multi-filament | 634 | 23.5 | 26.37 | R50/3 | 0.21 |

dramatic effect because of the high curvature induced in the fibre, **23J(8)**. Scales lift at the outer edge of the bend, and fracture commonly initiates at this outer edge and propagates inwards. Examination of the fractured ends showed that the crack had travelled across the fibre from the high tension zone on the outer side of the bend to the inner compression zone. Once in the compression zone, the crack tended to deviate along the fibre, leaving one side of the fractured end with a tapered end. Sometimes, this crack would deviate into a longitudinal (axial) split, due to the high shear stresses induced by these high curvatures.

## DAMAGE IN STITCHED SEAMS by Janet Webster

*The final example of processing damage comes at the end of the garment manufacturing chain, and is based on the PhD thesis, Webster (1996).*

Damage, which results from sewing and from subsequent mechanical action, was examined in the materials listed in Table 23.1. The seams of stitch type ISO-301 were made with a Singer Centurion 210B needle feed machine at 120 stitches/minute. After preparing the test pieces, the effects of subsequent wear were simulated by up to 50000 extension and recovery cycles at a rate of 150 mm/min, applying 5000 cycles a day for 10 days in a direction parallel to the stitch line. The test pieces remained in the tensile test machine at zero load between each successive day. After completion of extension cycling, the fabrics were allowed to relax at 65% r.h. and 20°C, and were then extended to the point of first stitch break at 50 mm/min.

The first two pictures are of sewing threads in the knitted cotton fabric immediately after seaming. Polyester filaments, **23K(1)**, show surface damage, and the mercerised cotton thread, **23K(2)**, has surface splintering. The fabric can also be damaged by the action of the sewing needles: **23K(3)** shows breaks caused in a woven wool fabric after sewing with the continuous filament polyester thread. Such damage was found only in the immediate vicinity of the seam.

The next two pictures are after the extension cycling. The surface damage on the polyester filaments, **23K(4)**, from a seam in the woven wool fabric is more severe. Splintering of fibres from the spun polyester thread stitched into the knitted wool fabric is seen in **23K(5)**. The last picture, **23K(6)**, is a break of a fibre from the mercerised cotton thread after the extension to the first stitch break.

1 5 μm

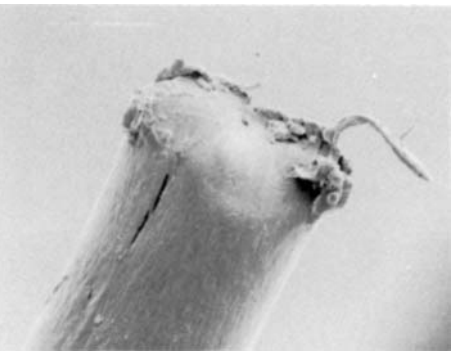

2 10 μm

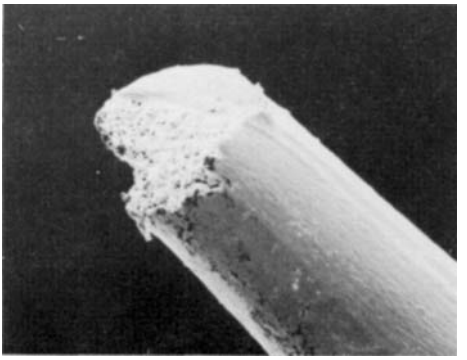

3 10 μm

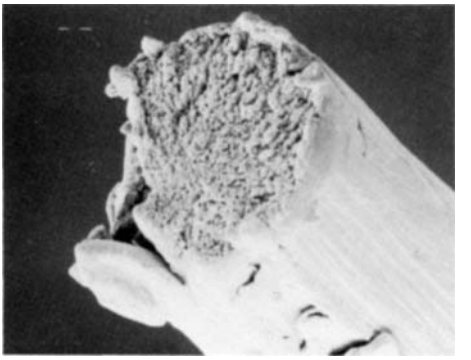

4 5 μm

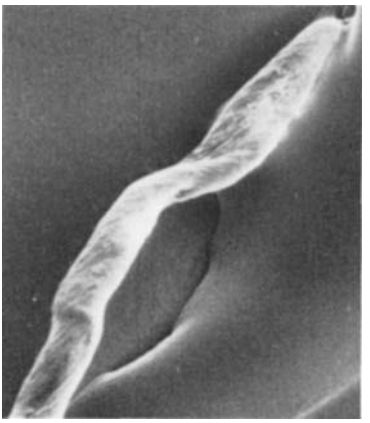

5 5 μm

6 10 μm

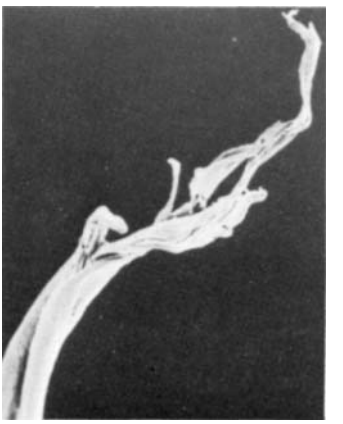

7 10 μm

**Plate 23A — Staple fibre ends.**
(1) Cut polyester. (2), (3) Cut acrylic. (4) Stretch-broken acrylic. (5) Tip end of cotton. (6) Root end of cotton. (7) End of cotton fibre damaged in processing.

1 ⊢—⊣ 100 μm

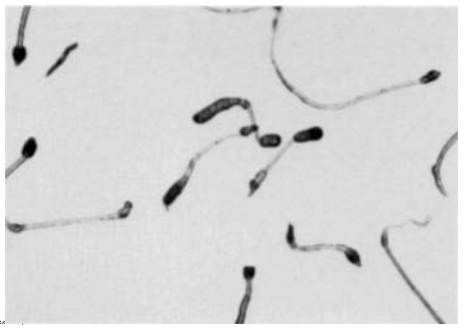

2

3a ⊢—⊣ 500 μm

3b ⊢—⊣ 200 μm

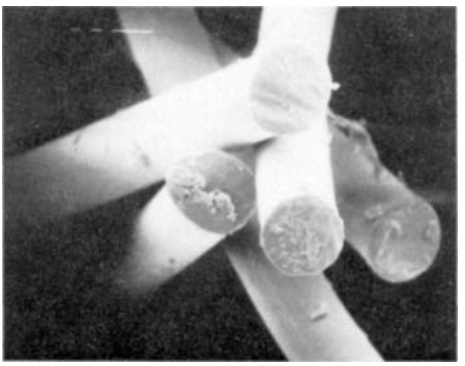

4 ⊢—⊣ 10 μm

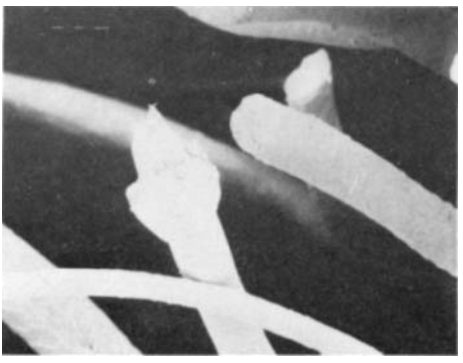

5 ⊢—⊣ 50 μm

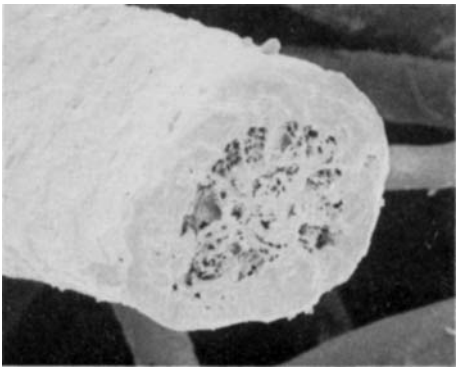

6 ⊢—⊣ 10 μm

**Plate 23B — Fabric singeing.**
(1) Tightly woven polyester fabric, made from ring-spun yarn. (2) Optical microscope view of short lengths of polyester fibres, singed at both ends, from a loose fabric made from open-end spun yarn.

**Fastener fabrics.**
(3a, b) Forms of projecting ends in different types of fastener fabric.

**Pile fabrics.**
(4) Fibre ends in polyester velvet. (5) From cut pile carpet (nylon and wool). (6) From cut pile carpet (wool), showing medulla.

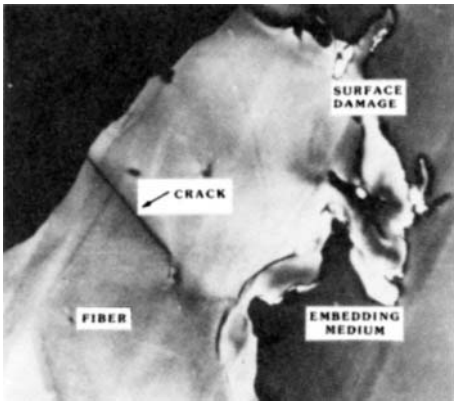


1

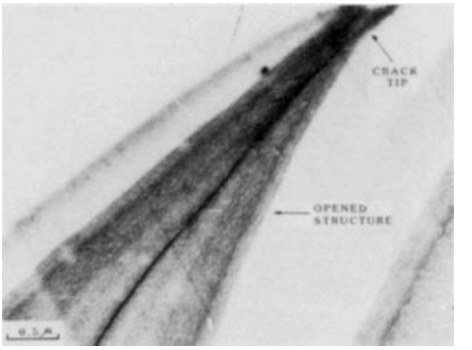


2

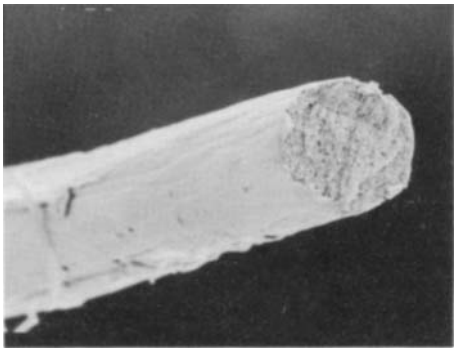

3

4

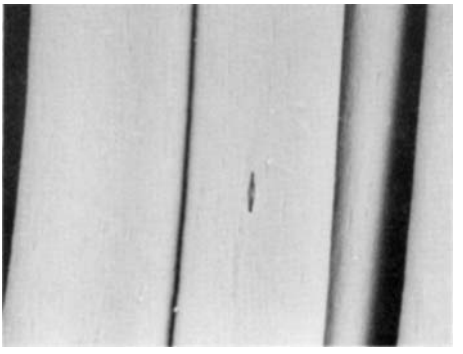

5

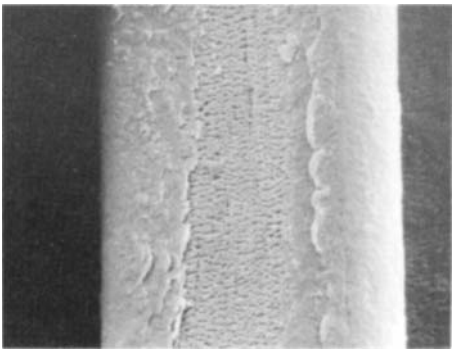

6

**Plate 23C — Transmission electron micrographs of stained sections of polyester fibres after carding, Davis (1989).**

(1) Low magnification view showing damage. (2) High magnification view showing opened structure round crack.

**Acrylic fibres from stretch-broken tow.**

(3) Granular fracture over single cross-section. (4) Break with multiple splitting.

**Polyester fibres treated with caustic soda.**

(5) Initial development of surface cracks. (6) More severe attack.


1

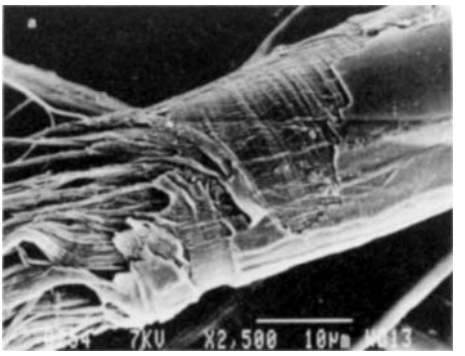


2

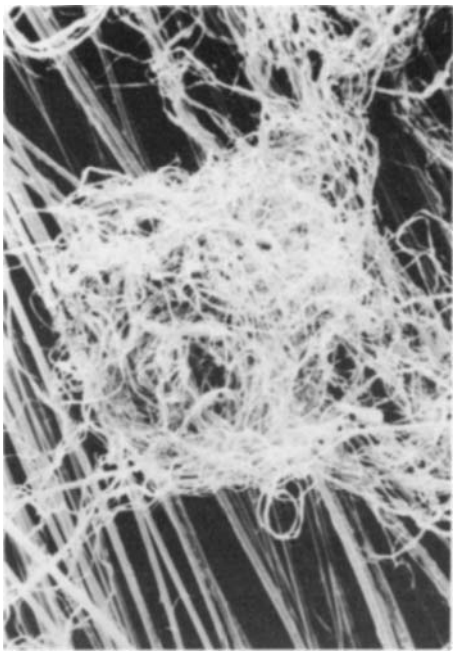

3

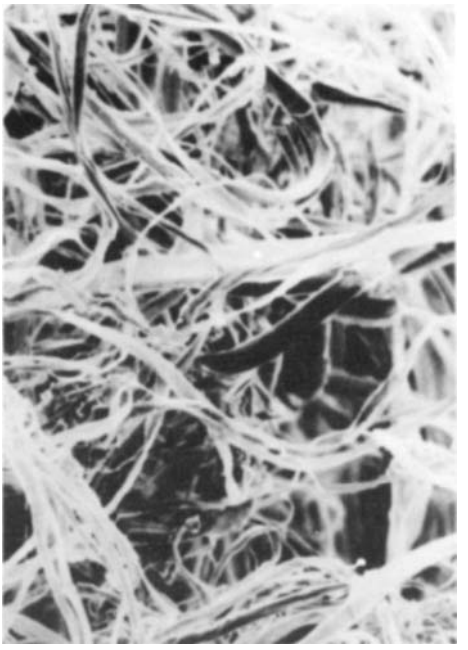

4

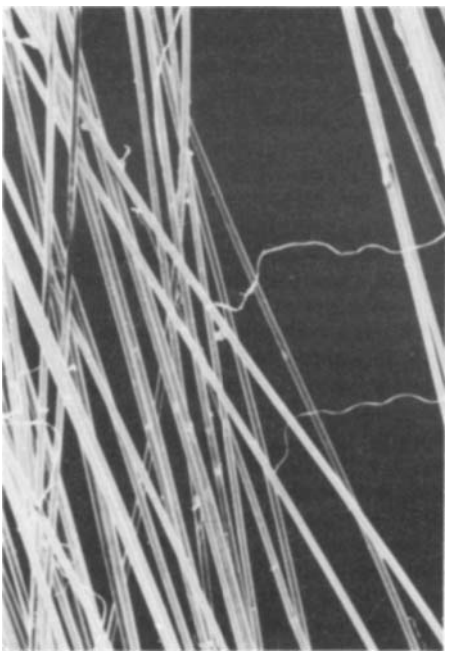

5

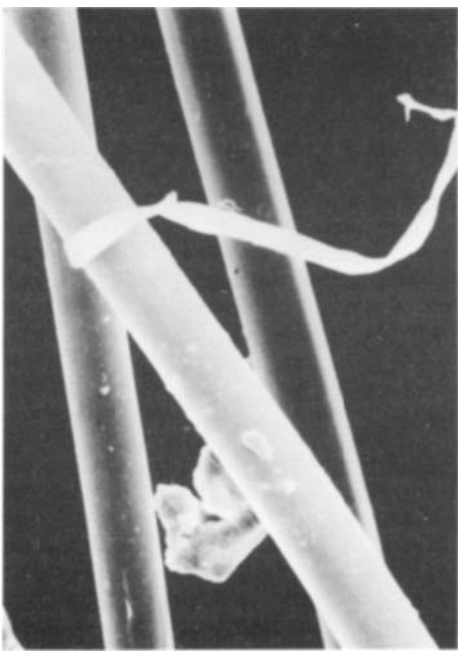

6

**Plate 23D — Beaten wood-pulp fibre, Hamad (1995).**
(1),(2) From pulp refined at 7.0 GJ/t, with partial removal of P and $S_1$ layers and exposure and disruption of $S_2$ layer (courtesy of A. Karnis, Pulp and Paper research Institute of Canada).
**Weaving damage in Kevlar aramid fabric, Greenwood and Cork (1984).**
(3),(4) Fibrillation in woven fabric. (5),(6) Unwoven yarn.

1

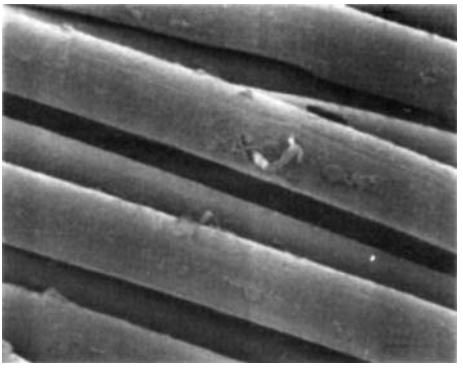

2

3

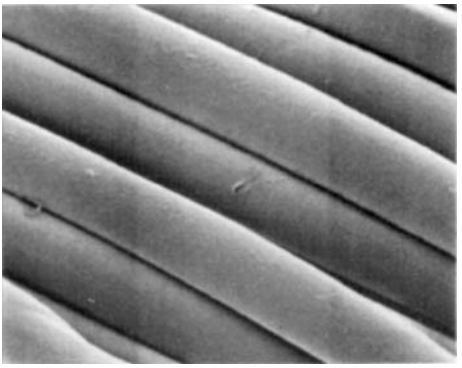

4

5

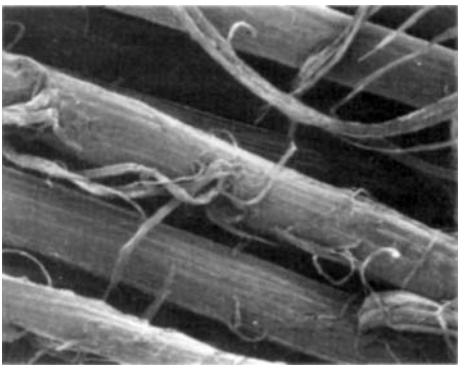

6

**Plate 23E — Courtaulds Tencel fibres in fabrics at various stages of processing, courtesy of T.R. Burrow, Courtaulds Fibres Tencel.**

(1),(2) Loomstate fabric. (3),(4) Singed and desized. (5),(6) Steam tumbled.

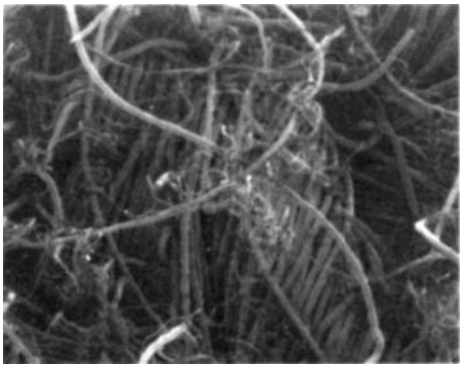

1

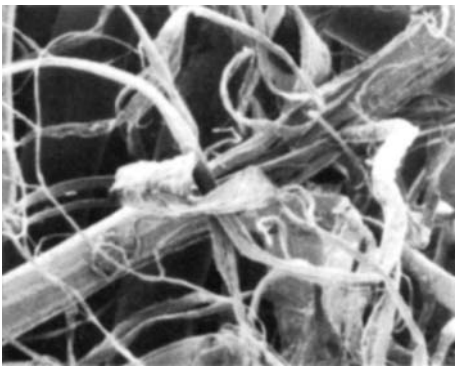

2

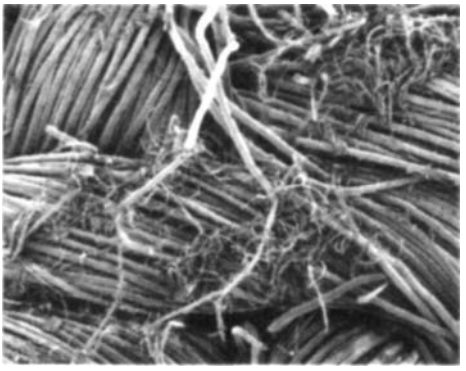

3

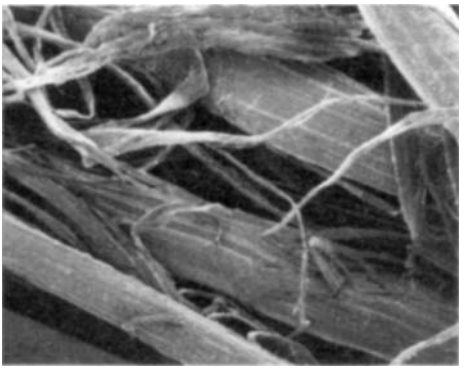

4

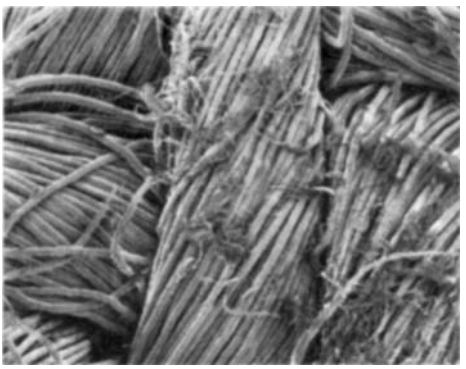

5

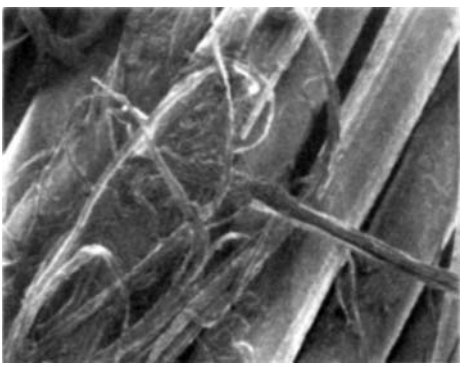

6

**Plate 23F — Courtaulds Tencel fibres in fabrics at various stages of processing, courtesy of T.R. Burrow, Courtaulds Fibres Tencel (continued).**
(1),(2) Prepared for beam dye. (3),(4) Set. (5),(6) Enzyme treated.

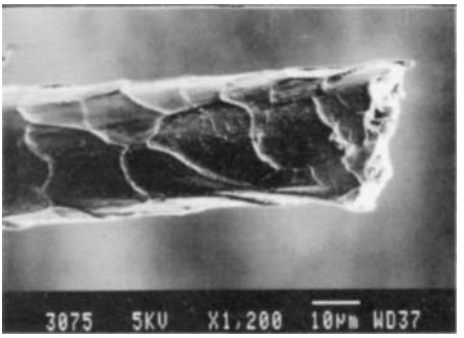


1

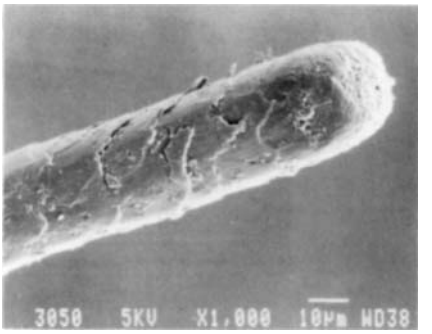


2

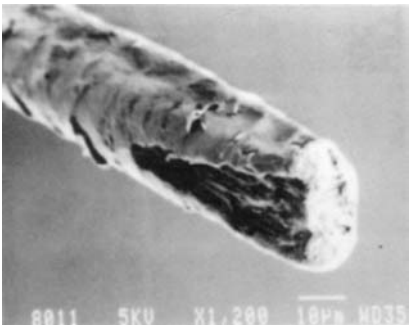


3

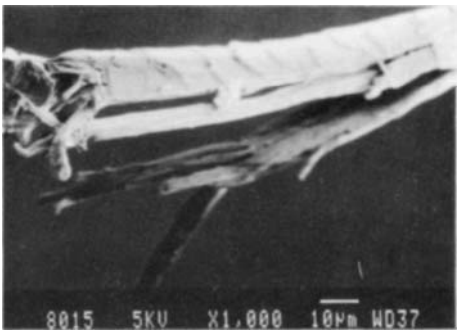


4

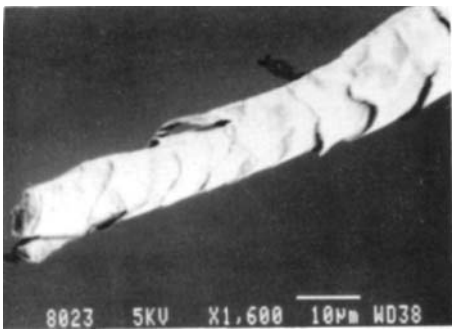


5

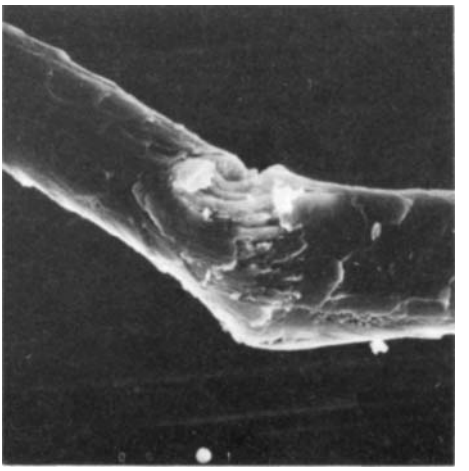

6

**Plate 23G — Studies of opening of wool.**
(1) A cut end for experimental studies. (2) Rounded end due to wear at 1000 m/min. (3) At higher speed. (4),(5) At 1860 m/min. (6) Incipient fibrillation.

1

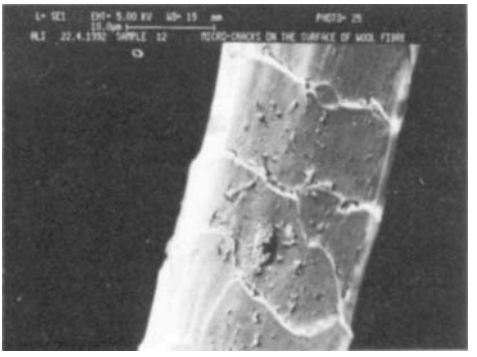

2

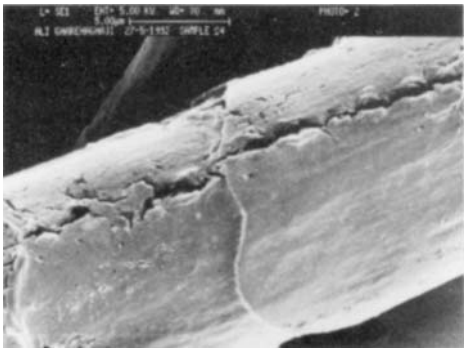

3

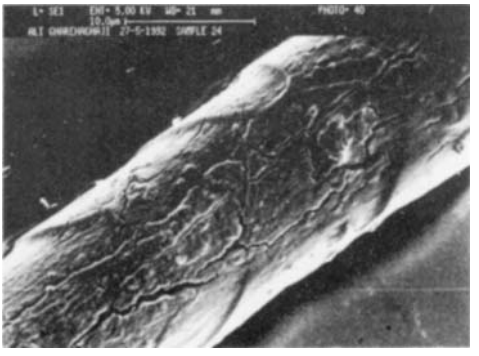

4

5

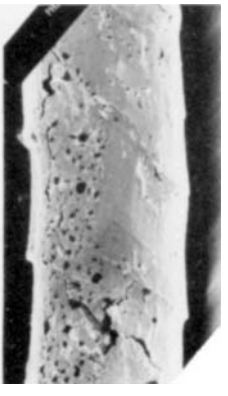

6

7

**Plate 23H — Studies of opening of wool (continued).**
(1) Surface wear and transverse cracks. (2) Transverse cracks at edges of scales. (3) Longitudinal cracks. (4) Joining of transverse and longitudinal cracks. (5) Deep cracks. (6) Clusters of holes. (7) Plastic deformation.

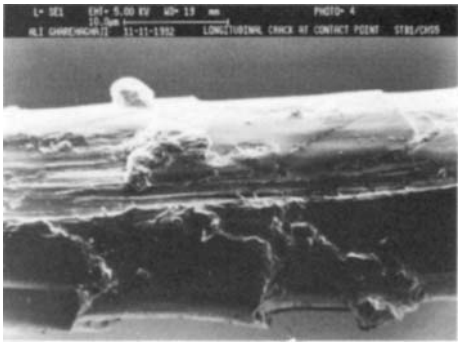

1

2

3

4

5

6

7

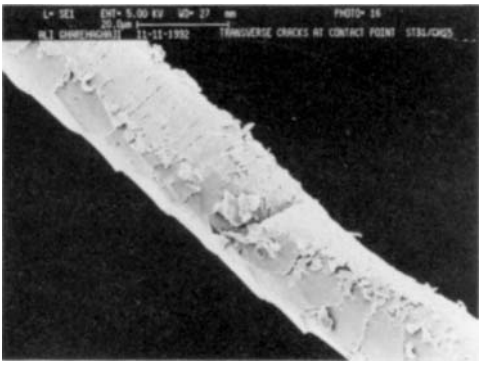

8

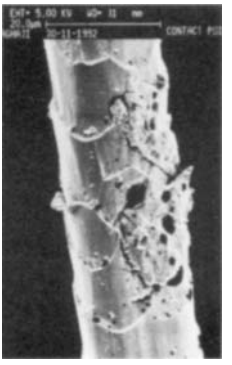

9

**Plate 231 — Wool pulled against opening elements in a tensile tester.**
(1) Axial splits, against wire. (2) Transverse cracks. (3)–(6) Plastic deformation. (7) Scale lifting. (8) Rippling and a cut. (9) Holes on fibre surface.

1

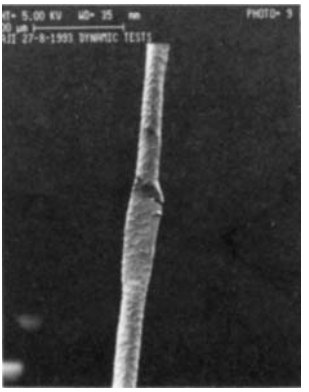

2

3

4

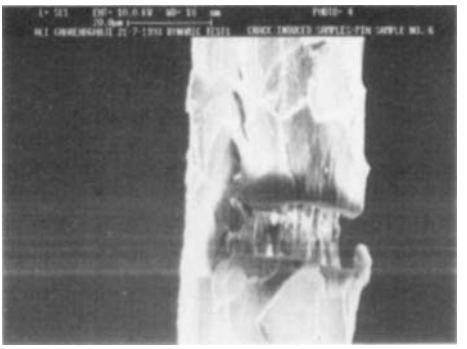

5

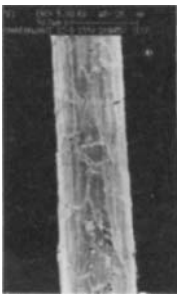

6

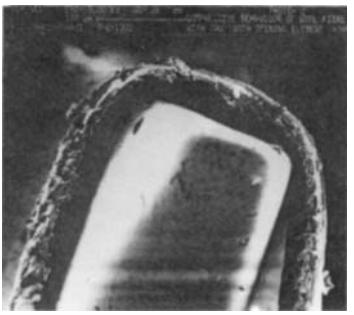

7

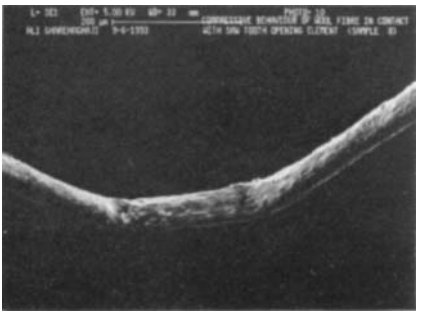

8

**Plate 23J — Fibres extended in SEM after opening damage.**
(1)–(3) Extension of a fibres that had been previously pressed against a sawtooth element. (4),(5) Crack and crazes. (6) Transverse crazes. (7) Wool fibre pulled against a sawtooth element in a live test in SEM. (8) Resulting plastic deformation.

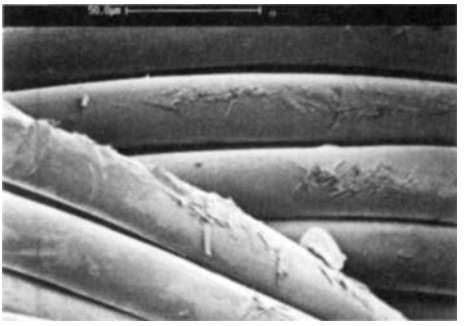

1

2

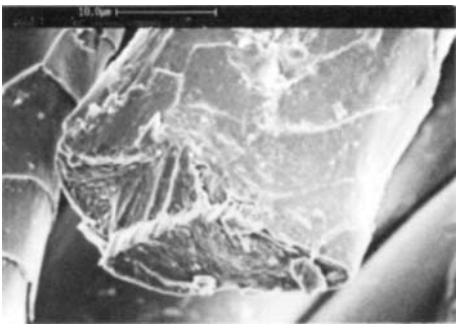

3

4

5

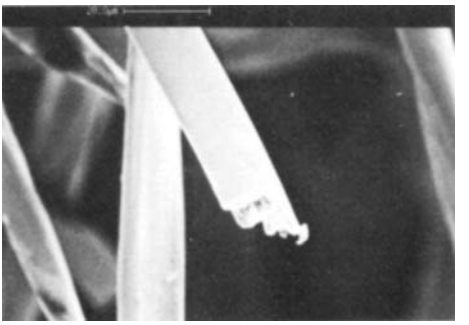

6

**Plate 23K — Damage from sewing and subsequent cycling, Webster (1996).**
(1) Continuous filament polyester sewing thread following seaming of knitted cotton fabric. (2) Mercerised cotton sewing thread following seaming. (3) Fibres from woven wool fabric in the vicinity of a seam. (4) Continuous filament polyester thread, sewn into woven wool fabric, after 50000 cycles between 20 and 25% extension. (5) Spun polyester thread. Sewn into knitted wool fabric, after 50000 cycles from 15 to 20% extension. (6) Mercerised cotton thread, sewn into knitted cotton fabric, after cycling from 10 to 15% extension and then extended to break.

# 24

# YARN TESTING

When drawn continuous-filament nylon or polyester yarn is subject to a tensile test in the form in which it is supplied to the industry, with only slight twist or interlacing, each filament breaks independently, and the fractured ends are the usual ductile breaks, with a V-notch and a catastrophic region, **24A(1), (2)**.

If the yarn is twisted, even to a fairly low level, transverse forces develop when the yarn is put under tension: these change the stress in the fibres, but also cause the filaments to act together. As soon as one fibre breaks, this triggers the break of the whole yarn. Some fibres, probably the first to break, show ordinary tensile breaks, **24A(3)**; in others the ductile form is recognizable but very distorted, **24A(4)**. But many fibres break with the appearance of high-speed tensile breaks, **24A(5),(6)**, as a result of the rapid transfer of load in the final stages of break.

The appearance of break of a highly twisted yarn is shown in **24B(1)**. The individual filament breaks now include some which can be regarded as ductile tensile breaks, albeit highly distorted, **24B(2)**, or as simple high-speed breaks, **24B(3)**. But it is also apparent that the large forces, which occur in twisting, have caused surface damage to the fibres, **24B(4)**, and that this has complicated the forms of break, **24B(5),(6)**, which include both mangling due to transverse pressure and splitting.

The presence of high-speed breaks among the filaments of a broken yarn, even though the extension was carried out slowly, is an important warning that the appearance of broken fibre ends from a fibre assembly can be misleading in regard to the real cause of failure. In an actual product there may be hundreds, or thousands, or even millions of fibre ends across the break; and the majority of these will have broken as a result of picking up the load in the final stages of break, which is of little interest since the damage has already been done. What is important is what starts the failure.

Another study of nylon yarn breaks has been reported by Ogata, Dougasaki and Yoshida (1979).

Yarns have also been tested in fatigue. In an attempt to overcome the difficulties of carrying out biaxial rotation fatigue studies on single cotton fibres, mentioned in Chapter 18, a study was made of testing yarns by biaxial rotation over a pin. The yarn structure does complicate the response, but the method is a useful one. When tested in air at 65% r.h., 20°C, the broken yarn ends thin down, but there are significant differences between ring-spun yarn, **24C(1)**, and open-end (rotor) spun yarn, **24C(4)**, with wrapped fibres being prominent in the latter yarn. The cotton fibres remain separate and show the usual biaxial rotation fatigue by multiple splitting, **24C(2),(3),(5)**. When tested in water the fibre structure tends to be smeared out, with sheets of material pulling away and sticking the fibres together, **24C(6)**. A similar effect is found after prolonged washing of cotton fabrics, as shown by examples in Chapters 32 and 34.

Another yarn test, illustrated in Fig. 10.6, was introduced as a means of evaluating resistance to surface sliding in continuous-filament yarns used to make ropes. Two portions of yarn twisted together are pulled backwards and forwards, so that they suffer abrasion against one another. It was found that there were two failure modes depending on whether the test conditions were mild, leading to a long life in the test, or severe, leading to a very short life. In 'slow' abrasion, for example with failure after 35 000 cycles, fibres break with considerable splitting, **24D(2)**, and get pushed back along the yarn to expose more fibres to abrasion, **24D(1)**. In 'rapid' abrasion, for example with failure in two cycles, there is a more localized and immediate failure, **24D(3)**, with squashed fibre ends and considerable complication of snap-back effects following breakage, **24D(4)**.

In conditions which are not as extreme as in the previous examples, in terms of giving very high or very low numbers of cycles to failure, individual fibres in yarns which have not been

taken to failure show extensive multiple splitting in mild conditions, **24E(1)**, but more squashing of the fibre under severe conditions, **24E(2)**.

The yarn-on-yarn abrasion test can be adapted so that the yarns are immersed in liquid, or preliminary treatments can be applied before testing. The most rapid breakage occurred with yarns which had been soaked in salt solution, or sea water, and then dried. The yarn damage is severe, **24E(3)**; and salt crystals, which are visible on the fibre surface, **24E(4),(5)**, presumably act as an abradant, gouging the fibres until they break, **24E(6)**. This is an important observation in regard to use of ropes and sails since although there is some difference, particularly in nylon, between fatigue resistance in wet and dry conditions, the really damaging situation is wetting and drying in a marine environment.

Detailed examination of fibre damage in yarn-on-yarn abrasion tests, except under very severe conditions, shows that the breakdown of nylon filaments mostly starts as peeling of strips from the fibre surface, **24F(1),(2)**, and develops into multiple splitting, **24F(3)**, as a result of the shear stresses. Similar effects are found in polyester filaments, **24F(4)–(6)**.

Under high tension the inter-fibre pressures can severely deform fibres, **24G(1)**, and this must be a factor in fibre breakage. However, even under relatively mild conditions, the fibres can be broken more by squashing than by splitting, **24G(2)**, and may be fused together, **24G(3)**. Possibly these effects occur in the later stages of the test, when the fewer filaments will be under higher tension. The occurrence of melting, **24G(4)**, and corrugating, **24G(5)**, is found in severe conditions, whether due to salt crystals or high tension. Finally, mushroom ends are found, **24G(6)**, but these probably form either when the load is rapidly taken up in the last cycle, which breaks the yarn, or are due to snagging of individual filaments. Some of the observed forms in **24G(3),(5),(6)** are probably a consequence of snap-back after break.

Many filaments are involved in yarn-on-yarn tests, and they are deformed, damaged and break in different ways at different stages of the test as the loading conditions on the fibres change. Then broken fibres tangle up, disturb the yarn structure, change the inter-yarn forces, and may themselves be further damaged. Thus the examination of broken yarns shows up a great complexity of forms, of which only a small sample has been illustrated here. The great distortions of the severe tests which lead to breakage in a very few cycles are perhaps of more academic than practical interest. But the surface peeling and multiple splitting, shown in **24F** and found in the milder conditions, is similar to that found in ropes, as shown in Chapter 39. The yarn-on-yarn abrasion test, carried out under the right conditions, is thus both a useful practical way of evaluating rope yarns, and a way of carrying out basic research on the surface shear and peeling mode of fibre failure, discussed in Chapter 14 and identified, rather loosely, as type 13 in Fig. 1.5.

Although yarns are an intermediate form, subsequently woven or knitted into fabric, there is some direct use of one-dimensional textile structures as braids, cords and ropes. A polyester braid was progressively load-cycled on an Instron strength tester from a base loading of 3% of its breaking load, with maximum loading increasing each cycle from 10%, 30%, 50% to 70% breaking load and then finally to break, which is shown in **24H(1)**. The break is complicated, with severe effects of snap-back, **24H(2)**. Most fibres have broken as high-speed breaks, **24H(3a)**, but some show other forms, **24H(3b)**, which are similar to tensile fatigue breaks.

If the braid is cycled for 1 hour between 3% and 70% of its breaking load prior to break, the broken filaments show evidence of melting, **24H(4)**, and there are interesting changes in fibre surfaces, **24H(5a),(5b)**. If the braid is cycled up to 90% of its breaking load, when it may fail after a short time, the surface damage is even more marked, **24H(6)**.

A nylon braid, fatigued to failure in water, is shown in **24I(1)**. There is evidence of surface peeling, **24H(2),(3)**, which would be due to surface rubbing, but other breaks, **24I(4),(5)** look more like tensile fatigue failure (see Chapter 11).

---

In **24D–G**, there are examples of yarn-on-yarn abrasion testing in continuous filament nylon and polyester yarns. Further tests have been carried out in which spun cotton yarns were subjected to yarn-on-yarn abrasion. When tested dry, **24J(1)**, the broken ends of fibres splay out from the yarn, and individual fibre ends show smearing wear with some fibrillation, **24J(2)**, or more extensive fibrillation, **24J(3)**. In the wet state, the intense smearing wear has caused the fibres to stick together in a mass, **24J(4)**. Individual fibres show some fibrillation, **24J(5)**, or complicated twisted forms, **24J(6)**.

The damage has similarities to that found in fatigue of cotton yarns by biaxial rotation over a pin, as shown in **24C**.

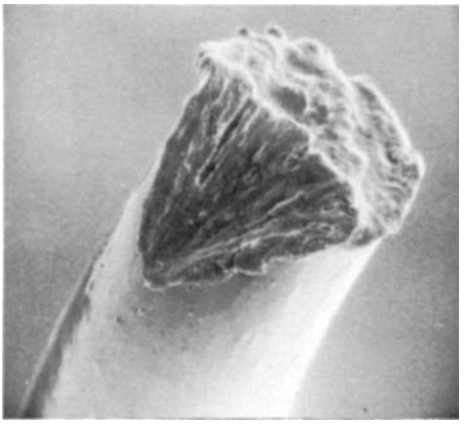

1 5 μm

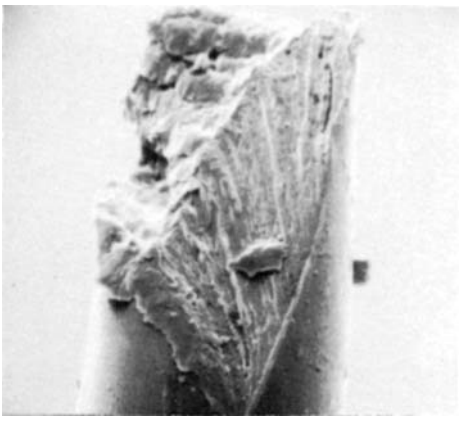

2 5 μm

3 5 μm

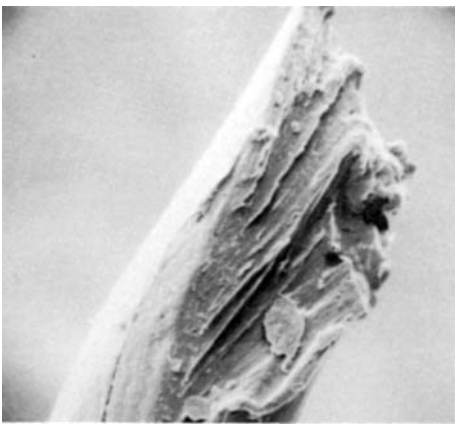

4 5 μm

5 5 μm

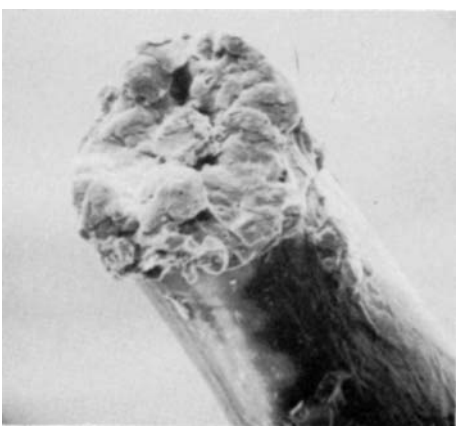

6 5 μm

**Plate 24A — Tensile breakage of 77 dtex/16-filament nylon.**
(1), (2) Filaments from yarn tested as supplied with little twist. (3)–(6) Filaments from yarn tested after insertion of 10 turns/cm.

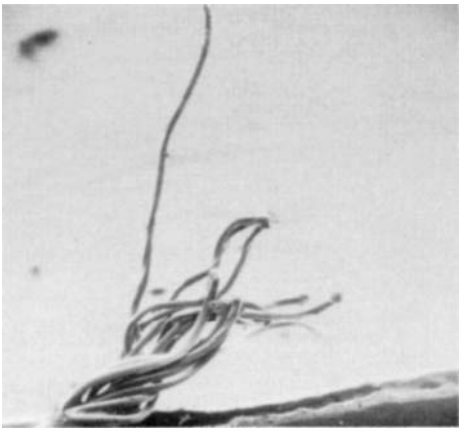

1 200 μm

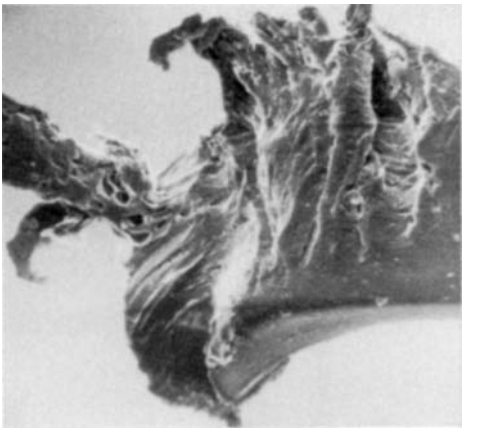

2 5 μm

3 10 μm

4 10 μm

5 10 μm

6 10 μm

**Plate24B — Tensile breakage of 77 dtex/16-filament nylon yarn, twisted to 100 turns/cm.**
(1) Broken yarn. (2)–(6) Individual filaments in broken ends.

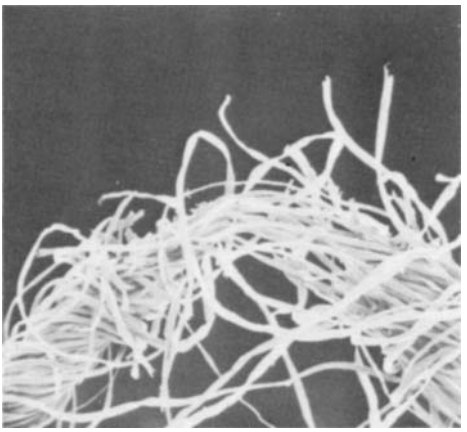

1 ⟷ 200 μm

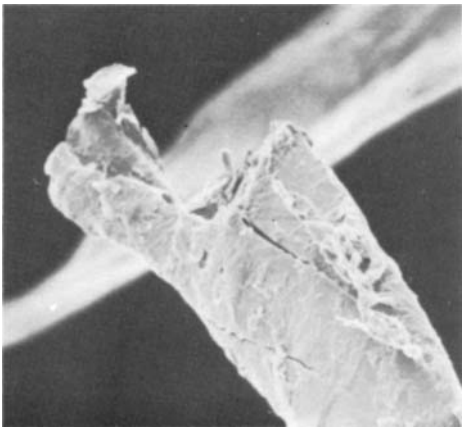

2 ⟷ 10 μm

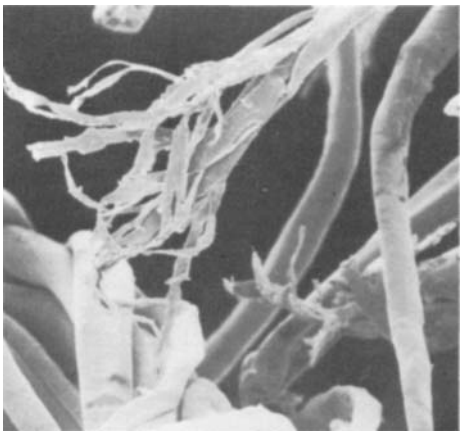

3 ⟷ 20 μm

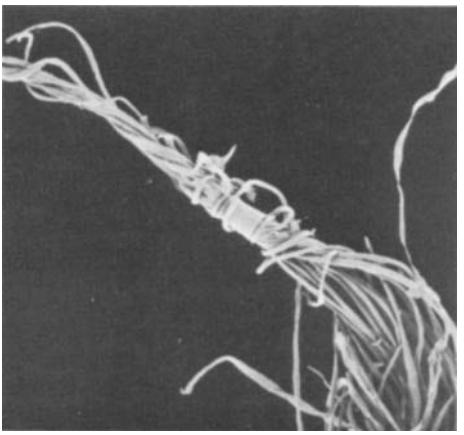

4 ⟷ 200 μm

5 ⟷ 10 μm

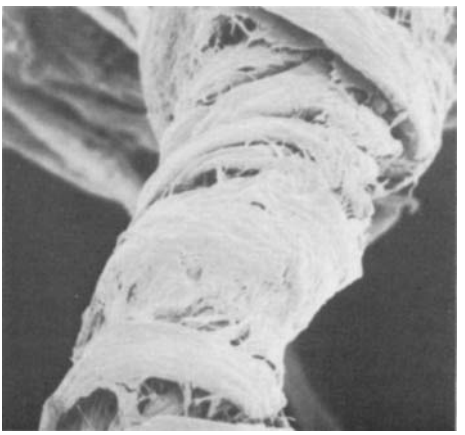

6 ⟷ 20 μm

**Plate 24C — Fatigue of cotton yarns by biaxial rotation over a pin.**
(1) Ring-spun untreated yarn, tested in air, after 4628 cycles. (2) Broken fibre from the yarn (1). (3) Broken fibre in mercerized ring-spun yarn, tested in air, after 4188 cycles. (4) Open-end spun untreated cotton yarn, tested in air, after 5311 cycles. (5) Broken fibre from the yarn (4). (6) Open-end spun untreated cotton yarn, tested in water, after 885 cycles.

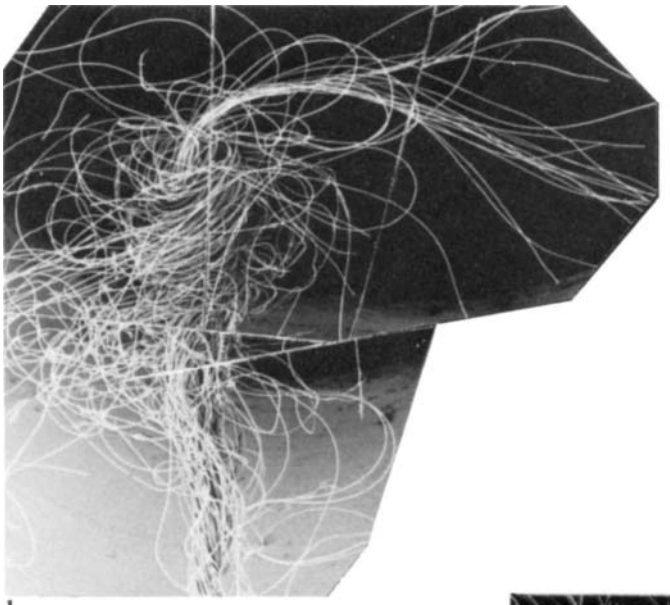

1

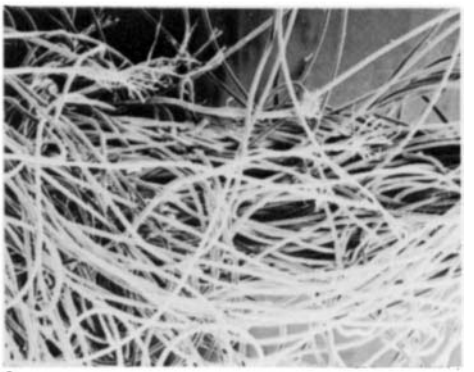

2

3

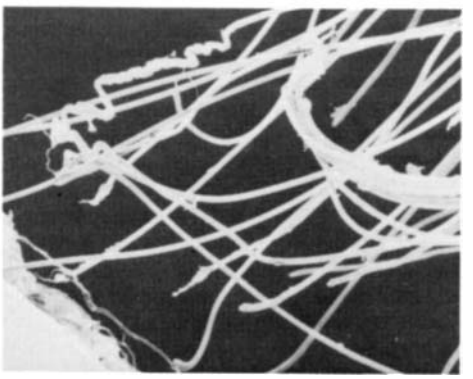

4

**Plate 24D — Yarn-on-yarn abrasion testing, 1100 dtex industrial filament yarns, three wraps at wrap angle of 35°, 50 mm stroke, 52 cycles/min, in air at 65%, 20°C.**
(1), (2) Nylon, with tension weight of 200 g, failed at 35 000 cycles. (3), (4) Polyester, with tension weight of 800 g, failed at 2 cycles.

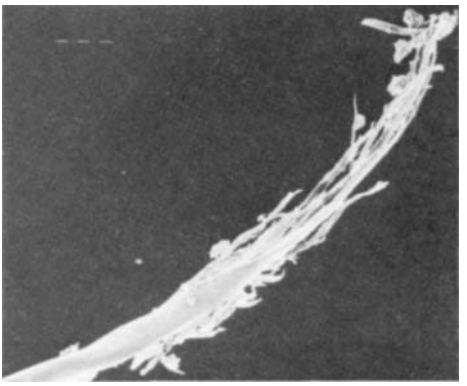

1 50 μm

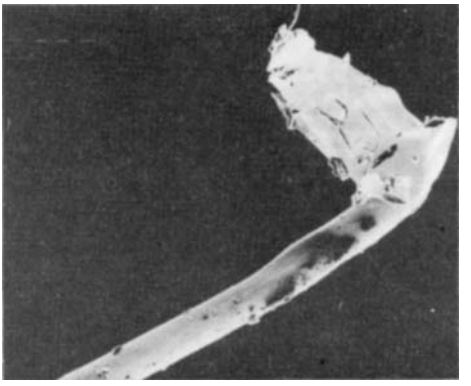

2 50 μm

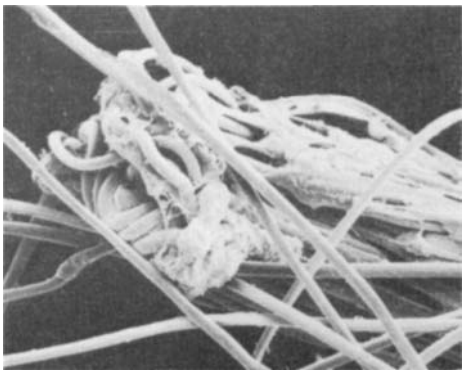

3 100 μm

4

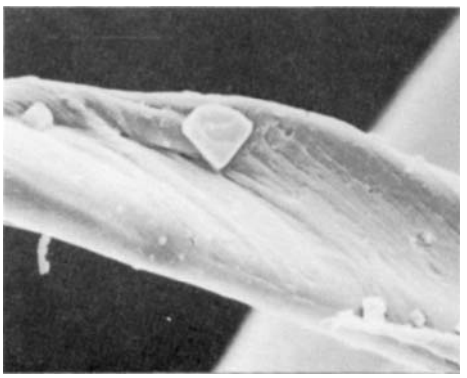

5 10 μm

6

**Plate 24E — Yarn-on-yarn abrasion testing: test conditions as in 24D.**
(1) Nylon fibre, from mild test, 500 g weight, after 3000 cycles, before yarn failure. (2) Nylon fibre, from severe test, 800 g weight, after 50 cycles, before yarn failure.

**Yarn-on-yarn abrasion of yarns soaked in sodium chloride solution and then dried: other test conditions as in 24D.**
(3), (4) Polyester, with tension weight of 400 g, failed in 41 cycles. (5) Nylon, with tension weight of 55 g, failed in 169 cycles. (6) Nylon, with tension weight of 500 g, failed in 93 cycles.

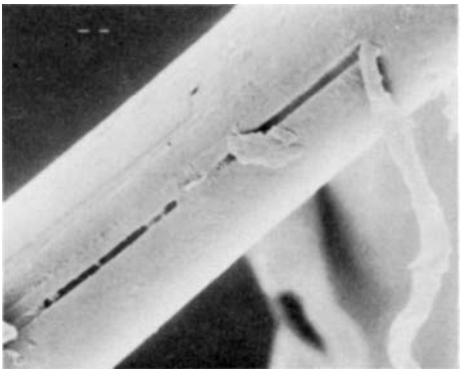

1 5 μm

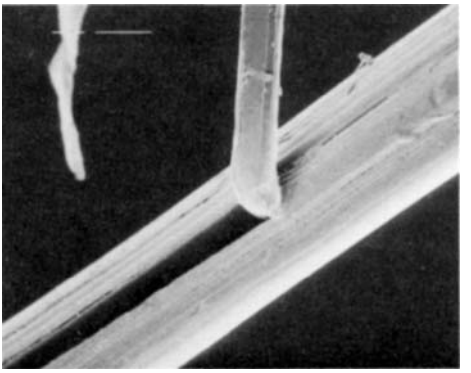

2 10 μm

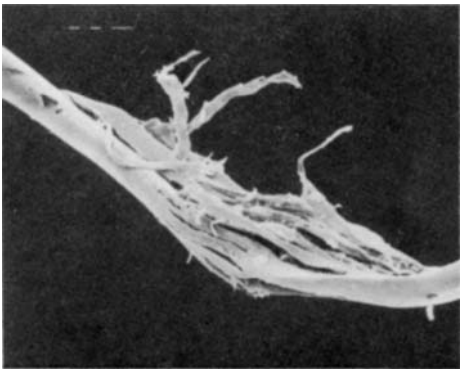

3 20 μm

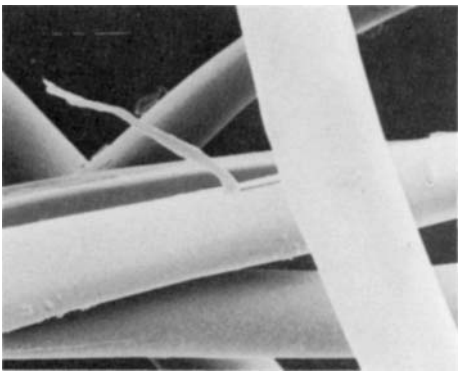

4 20 μm

5

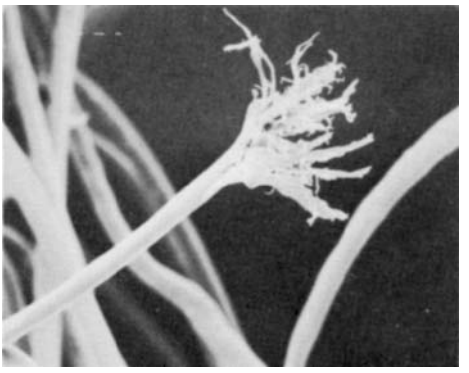

6 100 μm

**Plate 24F — Yarn-on-yarn abrasion testing in mild conditions: test details as in 24D (except as stated).** (1), (2) Nylon, with tension weight of 500 g, failed after 2600 cycles. (3) Nylon, with tension weight of 500 g, failed after 17000 cycles. (4) Polyester, with tension weight of 400 g, failed after 1600 cycles. (5) Polyester, with tension weight of 400 g, failed after 4900 cycles. (6) Polyester, with tension weight of 500 g, but lower wrap angle of 25°, failed after 13000 cycles.

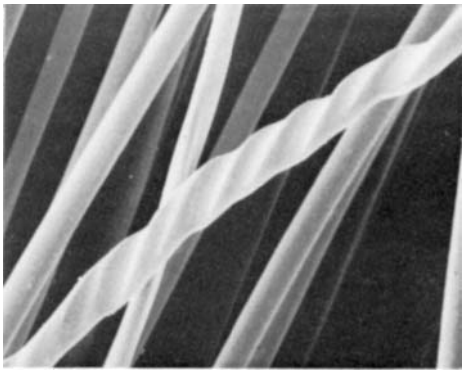

1

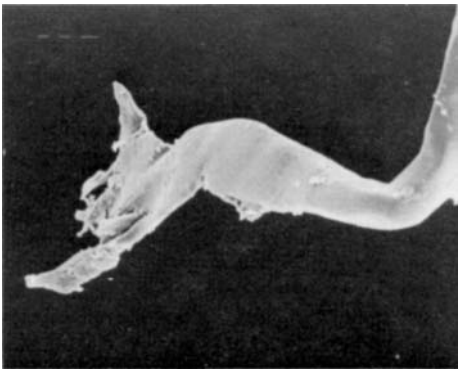

2 50 μm

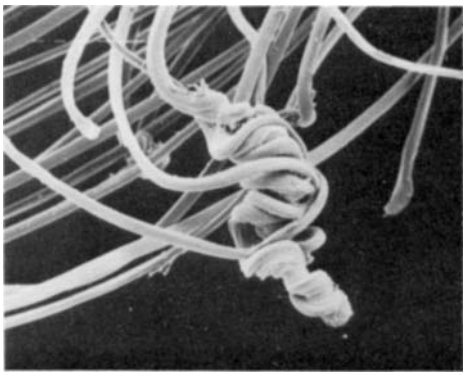

3 100 μm

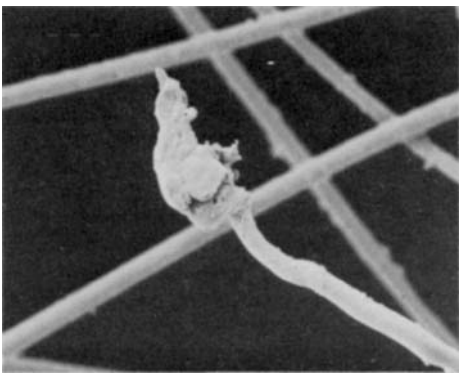

4 50 μm

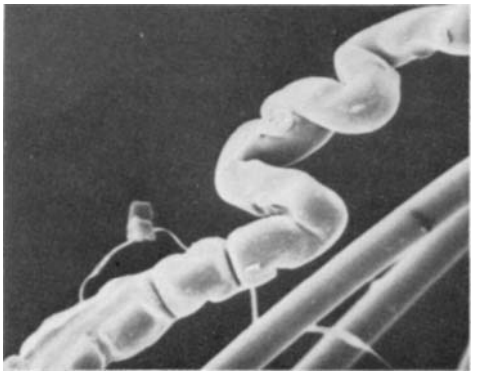

5

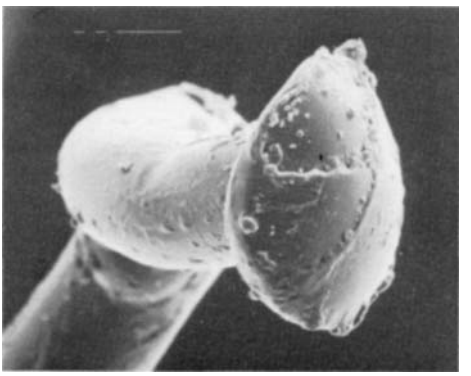

6 10 μm

**Plate 24G — Yarn-on-yarn abrasion testing: test details as in 24D (except as stated).**
(1) Polyester in water, with tension weight of 925 g, failed after 13 cycles. (2), (3) Polyester, with tension weight of 400 g, failed after 4800 cycles. (4) Polyester, dried from salt solution, with tension weight of 400 g, failed after 24 cycles. (5) Polyester, with tension weight of 800 g, failed after 2 cycles. (6) Polyester, dried from synthetic sea-water, with tension weight of 400 g, failed after 8 cycles.

1 ⊢—⊣ 500 μm

2 ⊢—⊣ 20 μm

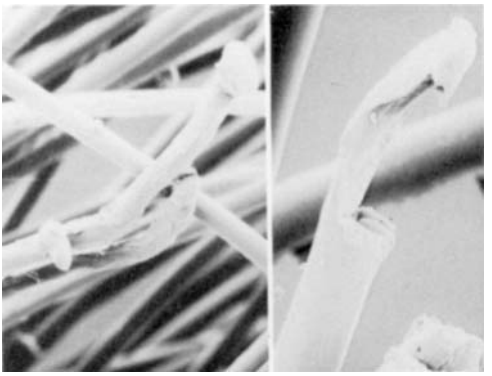

3a ⊢—⊣ 50 μm 3b ⊢—⊣ 20 μm

4 ⊢—⊣ 100 μm

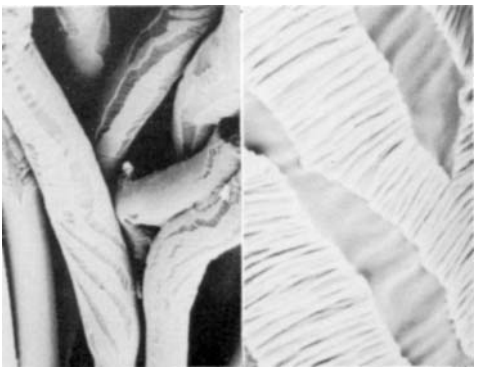

5a ⊢—⊣ 50 μm 5b ⊢—⊣ 5 μm

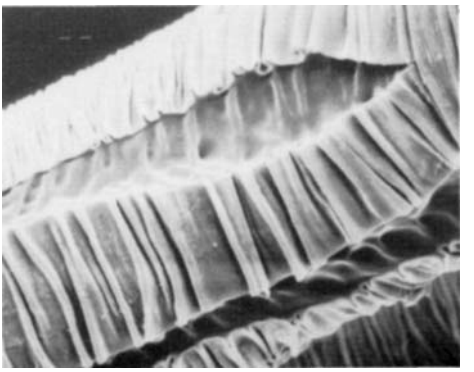

6 ⊢—⊣ 5 μm

**Plate 24H — Cyclic strength testing of polyester braid.**
(1) Broken end of braid. (2) Coiled filament, snap-back. (3a, b) Filament breaks. (4) Evidence of melting in break. (5a, b) Core softening, melting, splits and wrinkles. (6) Severe core melting and skin contraction.

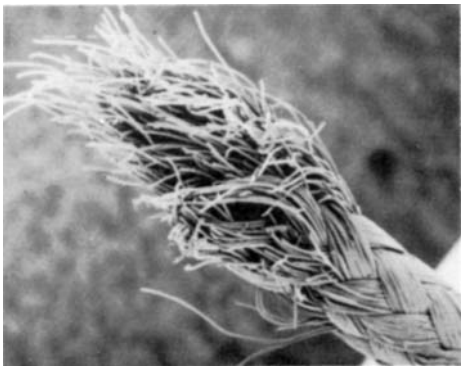

1 ⊢—⊣ 1 mm

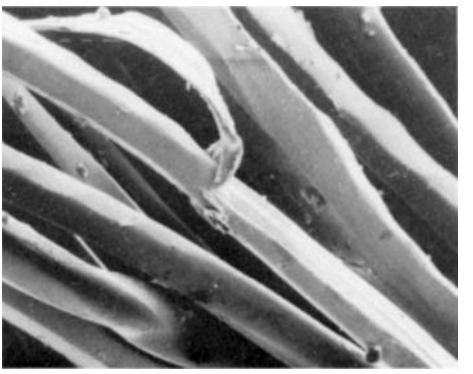

2 ⊢—⊣ 20 μm

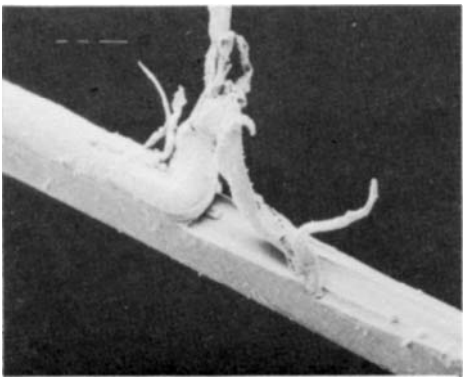

3 ⊢—⊣ 20 μm

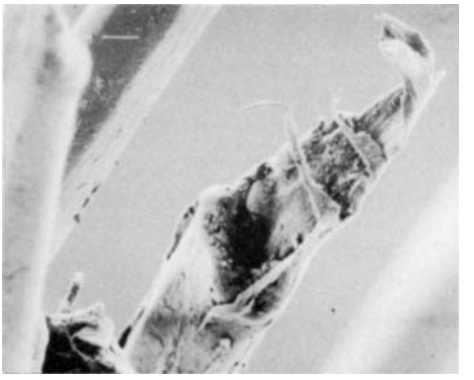

4 ⊢—⊣ 10 μm

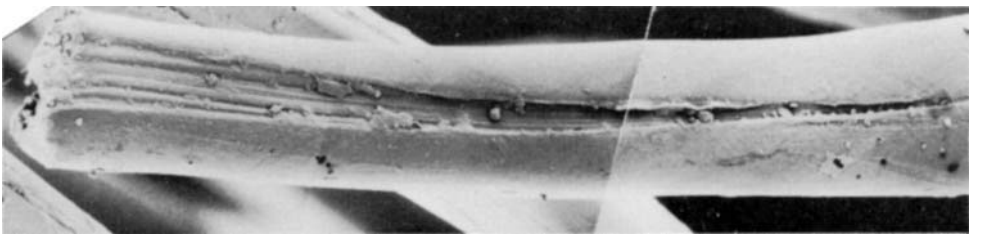

5 ⊢—⊣ 10 μm

**Plate 24(I) — Nylon braid fatigued tested in water, failed after 1374 load cycles.**
(1) Broken braid. (2), (3) Surface peeling of filaments. (4) Broken filament with tail. (5) Groove in broken filament.

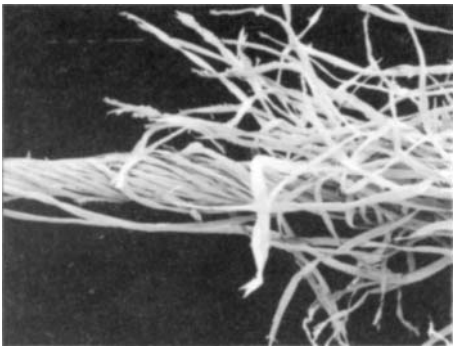

1

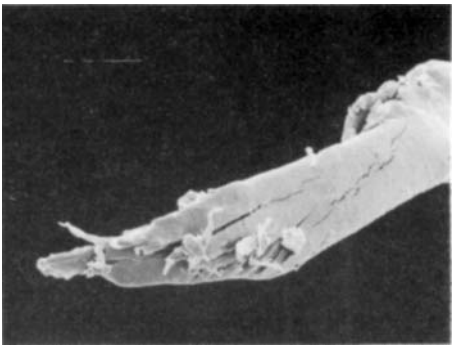

2

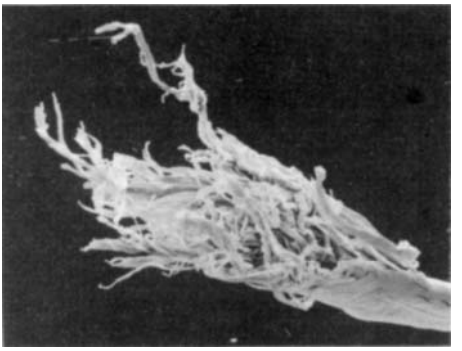

3

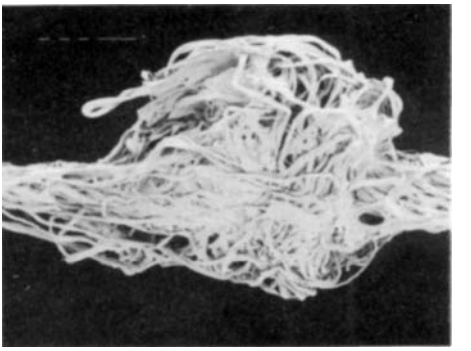

4

5

6

**Plate 24J — Cotton yarn-on-yarn abrasion.**
(1)–(3) Tested dry. (4)–(6) Tested wet.

# 25

# FABRIC TESTING

Until the early years of this century textiles were designed and evaluated on the basis of experience in use. But, once a more technical approach was established, one of the first types of laboratory test to be tried was fabric abrasion as a guide to wear in use. Often, in order to speed up the test, very severe conditions were employed. The correlations were rarely good, and then only for very limited changes in fabric specification, and were often badly misleading. Over the last 75 years many different wear-test devices have been suggested and used, but it remains difficult to get reliable and instructive information.

Detailed examination of the way in which damage occurs in abrasion tests provides valuable additional information. If the mode of breakdown is quite different to that found in real wear in use, then the test is not likely to be of much significance. If the forms of breakdown are similar, there is a chance that the information is meaningful. Apart from providing evidence on whether the lifetimes found in laboratory tests are likely to be a good guide to lifetimes in use, the detailed studies can help to elucidate the mechanisms of failure, and so lead to design improvements.

In studies using a WIRA abrasion tester with a standard worsted fabric abradant, a cotton fabric wore away at the yarn crowns, leaving fibre ends sticking up at the interstices of the weave, **25A(1)**, in a way similar to that found in use. The fibre breakdown of the cotton fibres in fabrics treated in three different ways — desize and scour, bleach and mercerize, dye and resin-treat — all show failure by multiple splitting, **25A(2)–(4)**, as found in single-fibre and yarn biaxial rotation fatigue and flex fatigue tests (Chapters 12, 13 and 24) and commonly in use. The break is somewhat sharper in the embrittled resin-treated material. Paper, whether rough or smooth, is a more severe abradant: it has a smearing effect on the fibres in the yarn crowns, **25A(5)**, and results in more rounded fibre ends, **25A(6)**, produced from the multiple split ends.

One of the problems of abrasion testing is that the abradant, as well as the test sample, suffers damage. The rough paper, **25B(1)**, becomes considerably worn away and smoothed after comparatively few rubs, **25B(2)**. The worsted fabric, **25B(3)**, also begins to break down, with fibre breaks by multiple splitting, **25B(4)**. The scales on the surface of the wool fibres, **25B(5)**, are worn away, **25B(6)**.

The many different types of laboratory abrasion tester operate in different ways, and it is beyond the scope of this book to describe them. But examples of the forms of damage are appropriate. See **25C**, which illustrates the effect of the Boss abrasion tester, **25C(1)–(3)**, the Martindale tester, **25C(4)**, the Stoll blade, **25C(5)**, and the Stoll bar test, **25C(6)**. All of these methods involve fairly high pressure on the fabric surface.

A recent addition to the KESF fabric testers, developed by Professor Kawabata at Kyoto University to evaluate fabric hand, is a shear fatigue tester, which involves no pressure on the surface. The fabric is repeatedly sheared in either direction, and thus breaks down as a result of internal action rather than an external abradant. A wool fibre in a fabric shows a multiple splitting in a portion from which the scales have broken away, **25D(1)**. However, comparatively little damage has been done, even after 100 000 cycles. The test can be speeded up by shearing the fabric wet with carborundum powder as an internal abradant: this leads to breakage of many fibres, **25D(2)**, but most of the damage is by direct abrasion on the fibre surface, **25D(3)**, although some fibres show multiple splitting fatigue, **25D(4)**. This form of severe damage would only be a realistic guide to the behaviour of a fabric if it was to be used in circumstances when it became contaminated with grit. Polyester fabrics show fibres with both multiple splitting, **25D(5)**, and surface peeling, **25D(6)**, presumably caused by surface shear.

There is an increasing use of rental companies to supply workwear on contract. These companies need to evaluate materials carefully and to monitor their use. This is a source of

valuable, well-documented samples for examination. Observations on material in use are included in Chapters 32 and 34, but the laboratory testing of fabrics was the source of the samples now described.

Fabrics abraded in the Accelerotor abrasion tester are shown in **25E(1)–(3)**. The polyester/cotton fabric tested dry shows heavy abrasion damage, with peeling and shredding of the cotton fibres, **25E(1)**, but shows little change from a control fabric after a test wet. Similarly a polyester/modal (rayon) fabric shows severe abrasion in the dry testing, **25E(2)**, but only slight abrasion and a few breaks of the rayon in the wet test, **25E(3)**.

The effect of the Martindale tester is somewhat different, as seen in the wear of a polyester/cotton fabric intended for protective clothing, **25E(4)–(6)**. There are many long bushy-ended polyester fibres on the surface, and broken cotton and polyester fibres in the crevices of the weave. The projecting polyester fibres can become tangled into pills on the fabric surface, which are held in place by a few anchor fibres (see Chapter 30). The multiple splitting of the polyester fibres can extend a long way back along the fibre, **25E(6)**.

In most contracts, wear resistance is only needed so that the garment does not become too worn, or weak, or unsightly to be usable, and repair of holes may be acceptable. But in the supply of all-over protective clothing for use in clean rooms, it is essential not only that the fabric shall prevent contamination coming from the wearer's clothing or person, but also that the fabric itself should not shed any fragments. A very high degree of wear resistance is therefore needed, and the fabrics must be thoroughly tested to make the right choice.

The results of abrasion of continuous-filament fabrics intended for clean-room garments are shown in **25F,G**, tested against a standard wool fabric by the rental company, and in a more severe test, when fabrics were abraded against themselves on a Martindale tester at UMIST for long enough (177 000 cycles) to cause damage.

A polyester (Dacron) taffeta, which has been surface-modified by calendering, showed almost no damage against wool, **25F(1a)**; but the self-fabric test causes light abrasion of the surfaces of some warp and weft yarns, **25F(1b)**, with splitting and peeling of filaments. The surface coating is broken in some places, and debris is trapped in the fabric. Near the edge of the test sample there was a line of severe damage, **25F(2)**, which may be at a crease in the fabric. Many of the broken filaments show typical multiple-split ends, **25F(3)**, but there is also some peeling, **25F(4)**, and the rounding of ends, **25F(5)**, which is a result of further wear after breakage.

Another polyester (Dacron) fabric in a herringbone weave had suffered slightly more damage in self-abrasion. Fibre breakdown appears to have started with surface peeling, **25F(6)**, with the fragments then piling up in the interstices of the weave. A few long fibre ends with bushy tips are present on the fabric surface.

In a nylon 6 (Celon) fabric, a few filaments have started to split even in the less severe abrasion against wool, and there was more pronounced splitting in the self-abrasion, **25G(1)**. There was an area of severe localized damage, **25G(2)**, probably at the edge of a crease, with multiple split fibre breaks sticking out.

In another surface-modified polyester (Terylene) fabric, the wear was worse. Against wool, filaments in the warp had broken, leaving the ends projecting from the fabric crevices, usually short but sometimes long, **25G(3a),(3b)**. In self-abrasion there is more breaking in the warp yarns, **25G(4)**, and the material in the crevices has become compacted together, **25G(5)**.

There was also severe damage in an uncalendered polyester fabric, with many broken ends in the abrasion against wool, and in self-abrasion, **25G(6)**. The fibre breakage is by multiple splitting. In this material the crimp in some filaments gives a looser packing, which may be beneficial for comfort but makes abrasion damage easier.

A situation in which it is justifiable to use a severe abrasion test is in the evaluation of webbings used in harnesses, rucksacks and similar situations where the webbing may be abraded by metal guides and buckles. An extensive set of tests was carried out by RAE, and samples became available for examination. The webbings were of nylon in a twill weave, with one type woven on a conventional loom with two conventional selvedges, and one on a shuttleless loom with one conventional selvedge and one tucked-in selvedge. These different selvedges influenced the abrasion resistance of the edges of the webbing. After 10 000 cycles of edge-abrasion, on a Hexbar tester, the conventional webbing had lost 40% of its original strength, whereas the shuttleless variant had lost only 2%.

Wear on the surface of the webbings appears similar in the two webbings, and in shown for conventional webbing in **25H(1)** in a zone where the interaction of yarn and fabric geometry is such that the filaments lie parallel to the length of the webbing. At higher magnification it can be seen that there is considerable flattening and smearing on the yarn crowns, **25H(2)**, which is a result of material being peeled off the surface of the fibres, **25H(3)**. In other locations the interaction of yarn twist and weave is such that the filaments are at an angle to the length of the fabric. This alters the topography of the webbing surface and leads to some difference in the nature of the wear, **25H(4)**.

Part of the selvedge of the conventional webbing showed considerable abrasion, with filaments twisted into loops and abraded, **25H(5)**. Damage to the filaments involved surface peeling, **25H(6)**. The shuttleless selvedge remained intact, even though it had suffered wear, **25I(1),(2)**. Damage to filaments depended on their location in the structure. The locking yarns of the weft showed failure by multiple splitting, **25I(3)**, but on the warp crowns scraping and

peeling of filaments was the dominant effect, **25I(4)**, and filaments were broken by flattening and shearing, **25I(5)**. In one region of very severe damage to the variant webbing, many fibres had been broken, **25I(6)**.

Another form of fabric testing is for flammability, or, more generally, the effects of heat on textile materials. SEM studies have been reported by Goynes and Trask (1985, 1987) for cotton, polyester and wool fabrics, including blends, with and without flame-retardant treatments, subjected to 45° edge ignition tests. A typical test specimen is shown in **25J(1)**, with an area burnt away at the bottom, and the residual piece consisting of a completely charred area, surrounded by an unburnt area, with an intermediate zone between these two, where heat will have had some effect on the fibres.

A comparison of unburnt and burnt untreated cotton twill is shown in **25J(2)**. There is shrinkage on burning, and the wispy, fragile charred material shows severe distortion of the cotton fibres, **25J(3)**. When the cotton fabric had been treated with a THPS finish, containing bis[tetrakis(hydroxymethyl)phosphonium] sulphate, urea and trimethylolmelamine, in a way which distributed the flame retardant throughout the fibres, the burnt region was black and brittle, but the fabric structure was little changed, **25J(4a)**. The cotton fibres retained their external shape, **25J(4b)**, although cross-sectional views showed that they had become thin-walled with enlarged lumens in the centres.

After burning an untreated 50/50 cotton/polyester fabric, there was little shrinkage, the char was less fragile than for 100% cotton, and, at low magnification, the appearance was similar to the treated cotton in **25J(4a)**. At higher magnification the mixture of fibres can be seen in the unburnt fabric, **25J(5a)**, but, in the burnt fabric, the cotton is coated with fused polyester, **25J(5b)**. Some distance away from the charred area the polyester fibres have started to melt; and there is a gradual progression from fused ends, similar to those shown in **20D(1)–(3)**, through larger regions of melting, seen in **25J(6a)**, to areas of complete embedding of the cotton fibres in the polyester melt, shown by the yarn cross-section in **25J(6b)**. The chars produced in burnt THPS-treated cotton/polyester fabric were not much different from those of untreated material.

In 100% polyester or wool fabrics the burnt material was a fused mass with no retention of fabric structure. However, untreated 60/40 cotton/wool fabric gave charred regions, similar to the cotton/polyester fabric, although not as dense. In the unburnt region there is loss of scale and ballooning of the wool fibres, **25K(1)**, and in the hotter regions there is melting of the wool and coating of the cotton fibres, **25K(2)**. The visual effects in the THPS-treated cotton/wool fabrics were similar.

Study of a tri-blend fabric of 60/25/15 cotton/polyester/wool enabled the sensitivity of the different fibres to heat to be shown up. In the untreated material the first indication of damage well above the charred area consisted of melting of polyester fibre ends, **25K(3a)**. Closer in, the molten polyester formed droplets and flowed over the other fibres, **25K(3b)**. Still nearer to the heat, the wool fibres began to swell, lost the scale structure and ruptured, **25K(4)**.

The heated, but not charred, region of THPS-treated tri-blend fabric was similar in appearance to the untreated fabric. Detail of the damage to the wool fibres is shown in **25K(5a),(5b)**. There are some differences in the charred remains, **25K(6a),(6b)**, but both untreated and treated fabrics have the charred cotton fibres embedded in the melted polyester/wool residue.

A number of general studies of fabric testing have been included in this chapter. Some more specific examples, which relate to particular products, such as rental textiles (Chapters 32 and 34), carpets (Chapter 33), seat belts (Chapter 37) and ropes (Chapter 39), are better brought into the accounts of case studies in use.

---

A series of fabric tensile tests were carried out by Seo *et al* (1993) in order to determine how failures differed according to the spinning technology used to make the yarns. **25L(1)** shows breaks starting in isolated places in a twill fabric before the rupture of the whole specimen. The fabrics had been piece dyed and the local failure exposed some relatively undyed material, so displaying the break as a light streak. Yarn breaks were of two types. In **25L(2)**, the break occurs sharply over a short yarn length. This reflects *extremely local load sharing of constituent fibres facilitated by high lateral pressures*, and the breaks usually occurred at bent configurations in crossovers. High lateral pressure is indicated by the deformed fibre ends in a yarn break, **25L(3)**. In some yarns, there were several bunches of fibre ends at intervals along the yarn, which are the sites of partial yarn breaks. The other type of break, **25L(4)**, has individual fibres breaking at many places over a considerable yarn length. The final separation occurs when the fibre lengths have become so short that they are no longer gripped and the fibre ends slip over one another.

Seo *et al*, who point out differences between ring, rotor and air-jet yarns, between plain and twill fabrics, and between warp and fill (weft) direction include among their conclusions:

*From observations of yarn failure in uniaxially tensioned fabrics, we see that in tests of fabrics in a displacement controlled test, there are numerous isolated yarn failures, accompanied by significant tensile load drop at each failure. In many cases, the magnitude of the load drop exceeded the average single yarn breaking strength.*

*Most of the isolated failures occurring in ring spun and rotor spun fabrics subject to warpwise loading originated at bend locations. These yarns tended to break abruptly, with few protruding fiber ends. . . . similar to the failure ends of yarns tested out of fabric at near zero gauge length. . . . Most isolated failures in ring spun fabrics tested fillingwise showed large amounts of long protruding fibre ends, leading to a long failure zone . . . similar to the failure ends of long gauge length yarns tested out of fabric.*

The form of tearing of fabrics depends on the tightness of the weave. This is shown in a study of the tongue tear test by Scelzo *et al* (1994). In loose weaves with high mobility, which is also accentuated by low friction and flexible yarns, the tear strength is higher and the tear is accompanied by major distortion of the fabric over an appreciable area, **25L(5)**. With tighter fabrics, allowing little yarn movement, the tear is sharper and the distortion is localised, **25L(6)**, with a lower tear strength due to the reduced fabric deformation energy.

The remaining pictures reinforce views elsewhere in the book. In ways similar to examples in Chapter 30, pilling, **25L(7)**, with breaks by multiple splitting, **25L(8)**, occurs in Martindale abrasion testing of a knit cotton fabric. The abrasion of a woven wool/mohair fabric is shown in **25M**. These pictures clearly display the concentration of wear at the interstices between yarns and the sequence from multiple splitting of fibres, due to bending, through a wearing away of the projecting ends while leaving the splits visible, to smooth rounded ends.

1 ⊢—⊣ 200 μm

2 ⊢—⊣ 10 μm

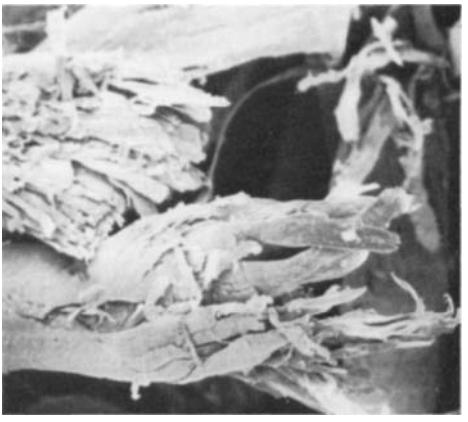

3 ⊢—⊣ 10 μm

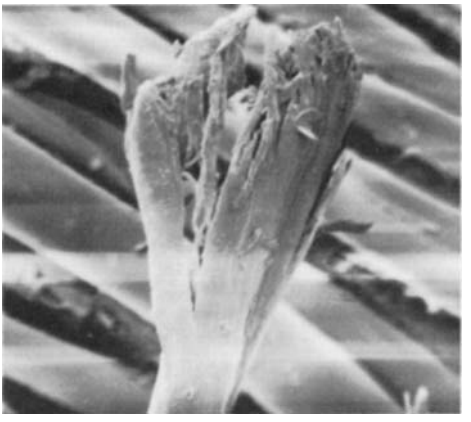

4 ⊢—⊣ 10 μm

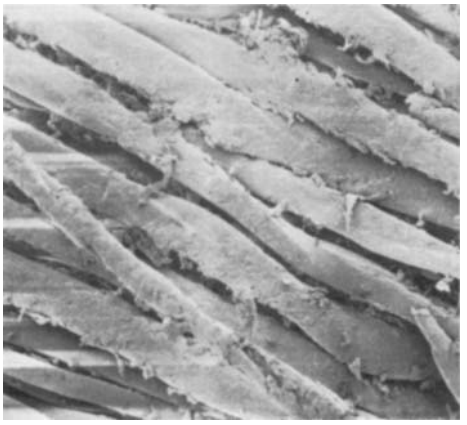

5 ⊢—⊣ 20 μm

6 ⊢—⊣ 10 μm

**Plate 25A — Laboratory abrasion of plain-weave cotton shirting fabric, 20 ends/cm × 20 picks/cm, on a WIRA abrasion tester.**

**Abraded against standard worsted fabric for 2000 rubs.**

(1) Bleached and mercerized fabric. (2) Fibre from desized and scoured fabric. (3) Fibre from bleached and mercerized fabric. (4) Fibre from dyed and resin-treated fabric.

**Abraded against paper**

(5) Dyed and resin-treated fabric against rough paper for 200 rubs: yarn crowns. (6) Fibres from dyed and resin-treated fabric against smooth paper for 300 rubs.

1 100 μm

2 100 μm

3 50 μm

4 20 μm

5 5 μm

6 5 μm

**Plate 25B — Damage to abradant in testing of cotton fabrics: test details as in 25A.**

(1) Rough paper before use as abradant. (2) Rough paper abraded against resin-treated cotton fabric for 200 rubs. (3) Worsted fabric before use as abradant. (4) Worsted fabric abraded against resin-treated cotton fabric for 2000 rubs. (5) Wool fibre from fabric before use as abradant. (6) Wool fibre from fabric after 2000 rubs.

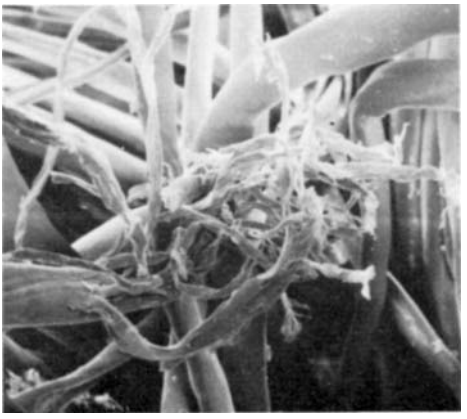

1 ⊢⊣ 20 μm

2 ⊢⊣ 20 μm

3 ⊢⊣ 5 μm

4 ⊢⊣ 20 μm

5 ⊢⊣ 50 μm

6 ⊢⊣ 5 μm

**Plate 25C — Effect of different abrasion testers.**
(1) Polyester/cotton sheet abraded on Boss abrasion tester using loomstate cotton canvas as abradant. (2) 48% cotton/52% rayon sheet Boss abraded with mineral khaki cotton canvas abradant. (3) Sheared-through viscose rayon fibre from Boss abraded cotton/viscose rayon sheet. Mineral khaki cotton canvas abradant. (4) 80% cotton/20% nylon sheet abraded on Martindale tester, standard crossbred wool fabric abradant. (5) Cotton sheet flex-tested against blade on Stoll tester. (6) Nylon fibre from cotton/nylon sheet flex abrasion tested on Stoll tester.

1 ⊢—⊣ 20 μm

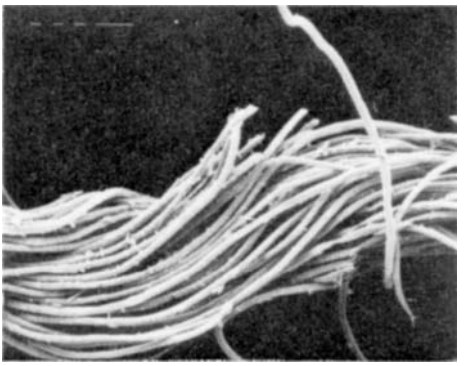

2 ⊢—⊣ 100 μm

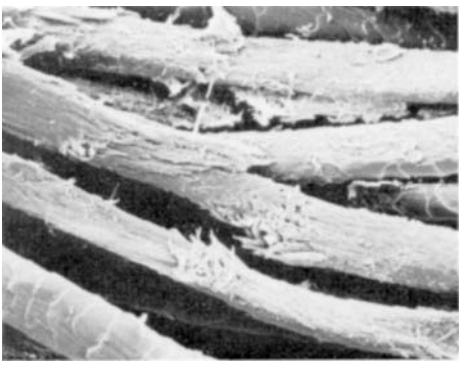

3 ⊢—⊣ 20 μm

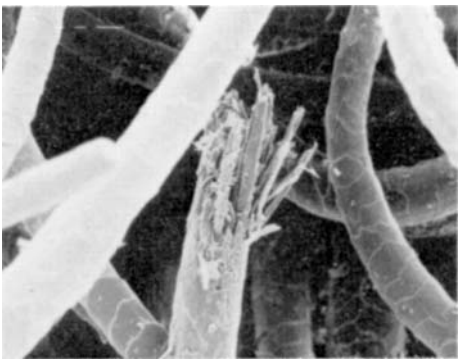

4 ⊢—⊣ 20 μm

5 ⊢—⊣ 20 μm

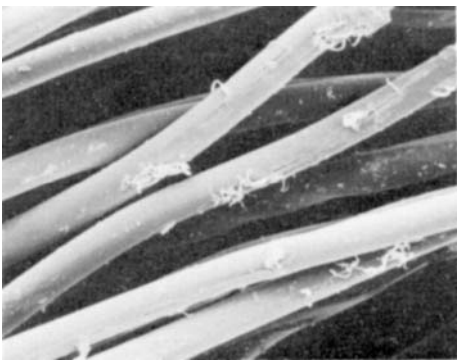

6 ⊢—⊣ 20 μm

**Plate 25D — Shear cycling of fabrics by Kawabata.**
(1) Wool fabric, after $6 \times 10^5$ cycles. (2) Warp yarn from wool fabric tested with carborundum and water, after $10^5$ cycles. (3), (4) Wool fibre damage after testing as in (2). (5), (6) Polyester fibre, after $10^5$ cycles.

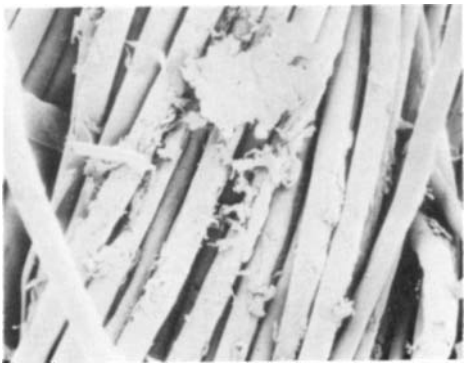

1 ⊢⊣ 20 μm

2 ⊢⊣ 10 μm

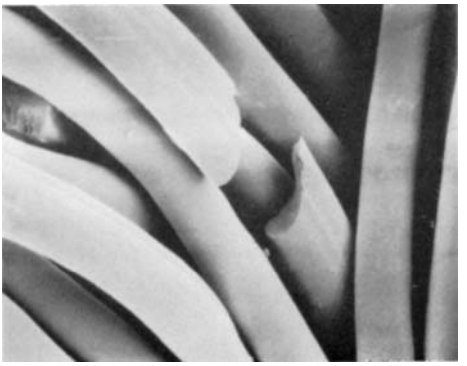

3 ⊢⊣ 20 μm

4 ⊢⊣ 1 mm

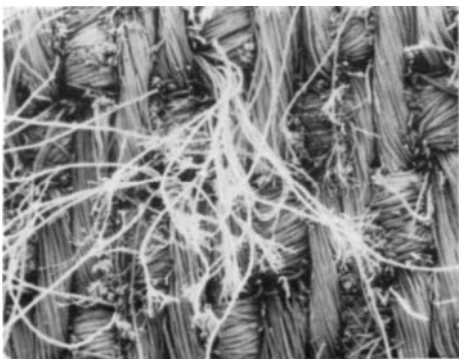

5 ⊢⊣ 200 μm

6 ⊢⊣ 50 μm

**Plate 25E — Abrasion testing of overall fabrics using Accelerotor tester.**
(1) Polyester/cotton fabric abraded dry; severe damage to cotton fibres in yarn crowns. (2) Polyester/modal fabric abraded dry; more of a cutting action on fibres. (3) Same fabric as in (2) but wet abraded in accelerotor. Break in modal fibre.

**Using Martindale tester.**

(4) Miraclean, polyester/cotton workwear after 75 000 rubs on Martindale. (5) Detail of fabric surface, as in (4). (6) Long bushy end of polyester fibre, as in (4).

1a ⊢⊣ 100 μm

1b ⊢⊣ 200 μm

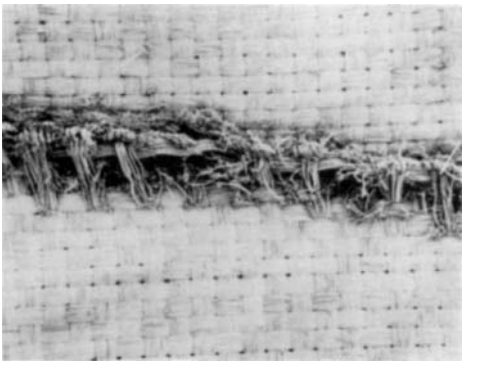

2 ⊢⊣ 1 mm

3 ⊢⊣ 200 μm

4 ⊢⊣ 50 μm

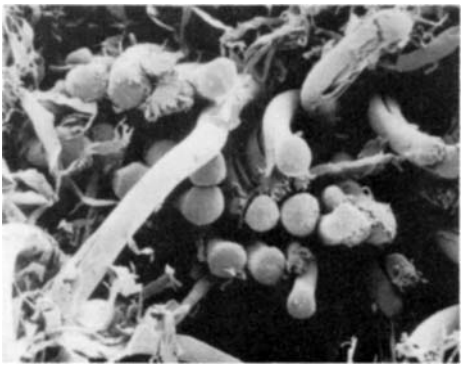

5 ⊢⊣ 50 μm

6 ⊢⊣ 10 μm

**Plate 25F — Abrasion testing of fabrics for clean-room garments: (a) less severe — against standard wool fabric by company; (b) more severe — against the test fabric itself for 177 000 cycles on Martindale at UMIST.**

(1a) Polyester (Dacron) taffeta, against wool. (1b) Same fabric, against self. (2) Same fabric, against self, line of severe damage, possibly at crease. (3)–(5) Details of wear of fibres in region of (2). (6) Polyester (Dacron) herringbone, against self, start of fibre peeling.

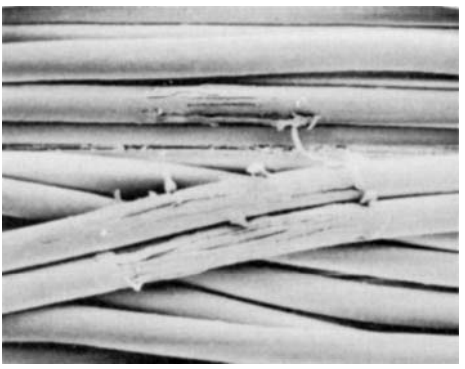

**1** 50 μm

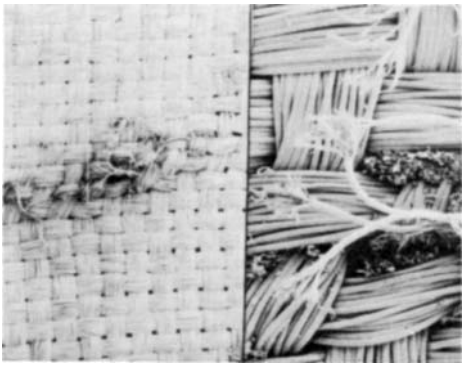

**2a** 1 mm **2b** 200 μm

**3a** 200 μm **3b** 100 μm

**4** 50 μm

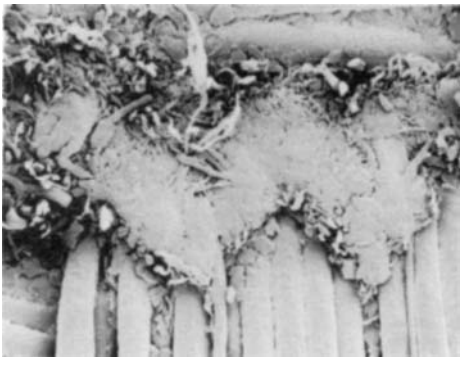

**5** 20 μm

**6** 100 μm

**Plate 25G — Abrasion testing of fabrics for clean-room garments (continued).**
(1) Nylon (Celon) fabric, against self, splitting of filaments at yarn crown. (2) Same fabric, against self, showing localized area of severe damage at edge. (3a,b) Polyester (Terylene) fabric, against wool, broken fibres at yarn interstices. (4), (5) Same fabric, against self, with compacting of broken fibres. (6) Partly textured yarn polyester fabric, against self.

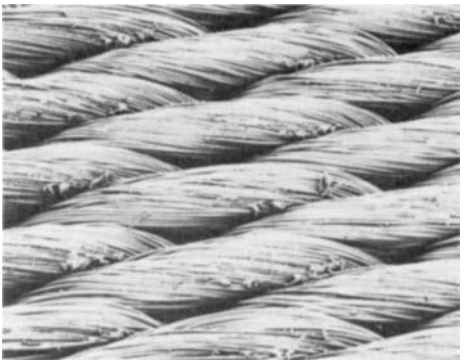

1 ⊢—⊣ 500 μm

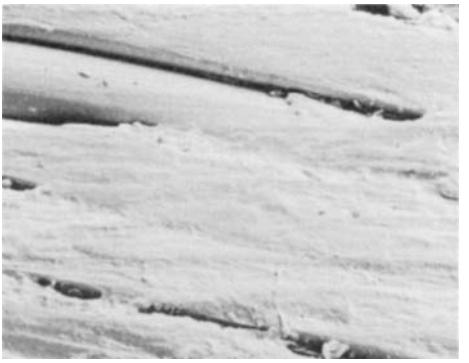

2 ⊢—⊣ 20 μm

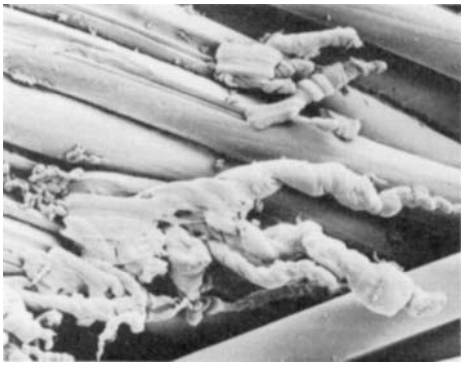

3 ⊢—⊣ 20 μm

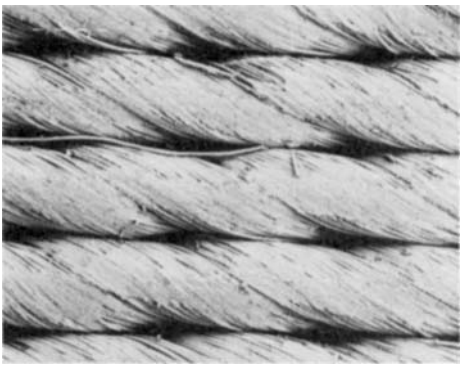

4 ⊢—⊣ 500 μm

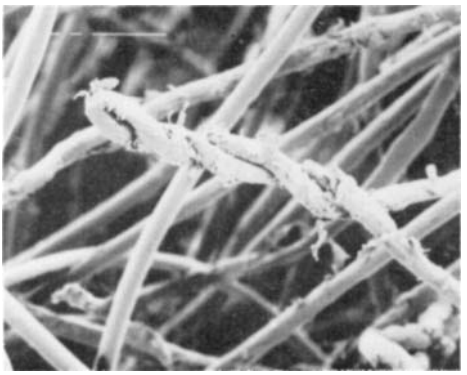

5 ⊢—⊣ 50 μm

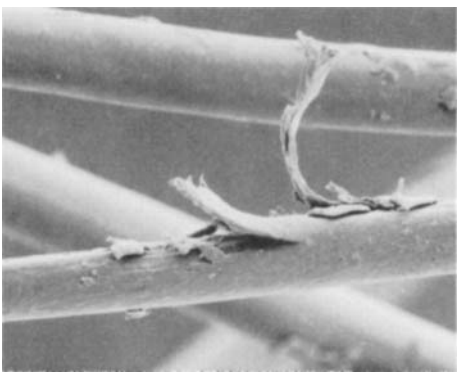

6 ⊢—⊣ 20 μm

**Plate 25H — Abrasion testing of nylon webbing by Hexbar.**
(1) Surface wear of conventional webbing. (2) Scraped surface of yarn crown. (3) Rolling-up of surface peels at end of crown. (4) Surface smearing and scraping at variant selvedge. (5) Twisted-up, abraded filament near top of conventional selvedge. (6) Peeled filament at top of damaged conventional selvedge.

1 1 mm

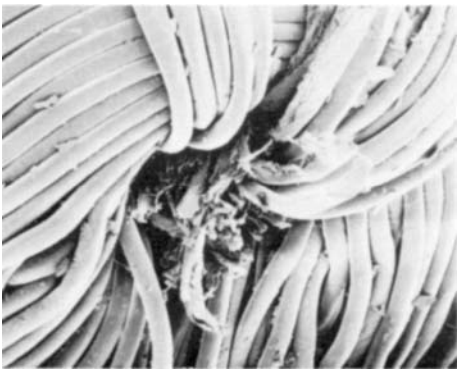

2 100 μm

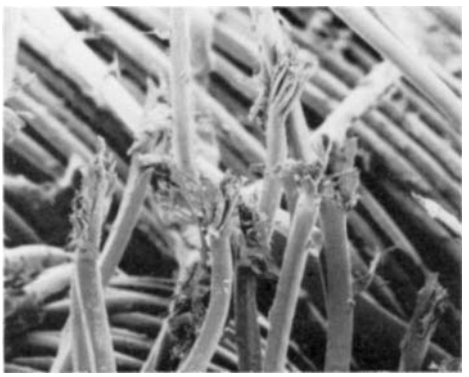

3 100 μm

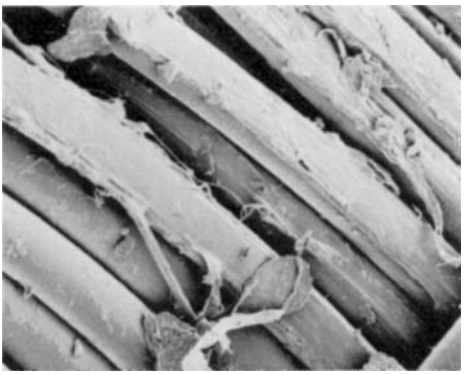

4 20 μm

5 50 μm

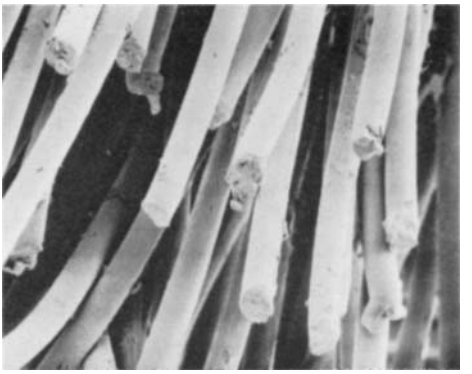

6 50 μm

**Plate 251 — Abrasion testing of nylon webbing by Hexbar (continued).**
(1) Damage to variant selvedge (non-conventional) after $10^4$ cycles against Hexbar. (2) Broken fibres in loop holding edge yarns of the selvedge. (3) Broken split ends in yarn lying along selvedge (edge of crown). (4) Surface peeling of yarn crossing over variant selvedge. (5) Sheared ends at variant selvedge. (6) Broken filaments at edge of variant selvedge.

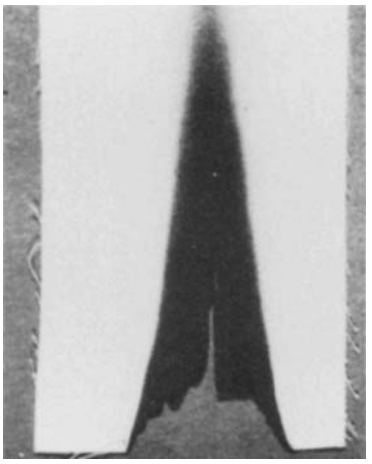

1

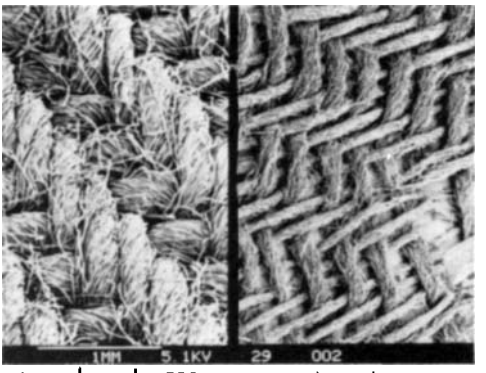

2a 500 μm 2b 500 μm

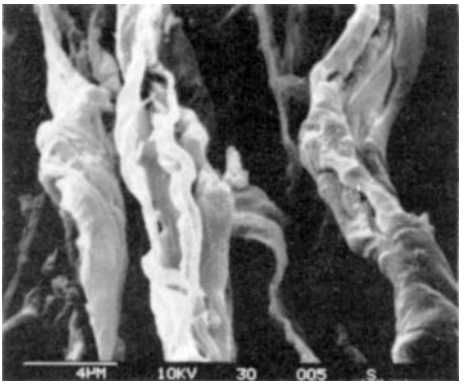

3 2 μm

4a 500 μm 4b 5 μm

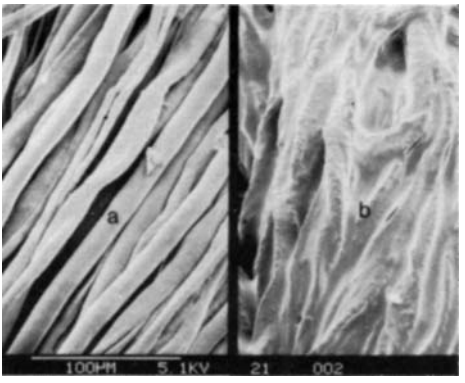

5a 50 μm 5b 50 μm

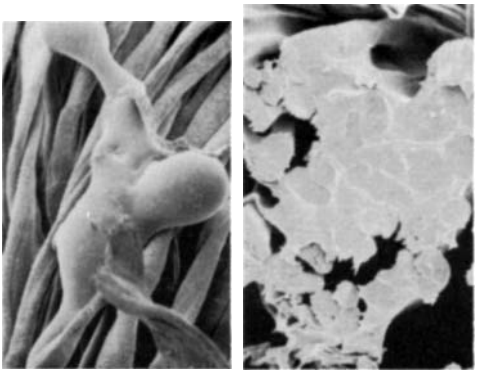

6a 20 μm 6b 20 μm

**Plate 25J — Fabrics after burning (from Goynes and Trask, 1985, 1987).**
(1) General view of test sample. (2) Comparison of (a) unburnt and (b) burnt untreated cotton fabric. (3) Charred untreated cotton fibres, from (2b). (4a,b) Charred THPS-treated cotton fabric, and enlarged view of fibres. (5) Comparison of (a) unburnt and (b) burnt untreated cotton/polyester fabric. (6a) Fused polyester fibres on fabric surface away from the charred region. (6b) Yarn cross-section with cotton in polyester melt.

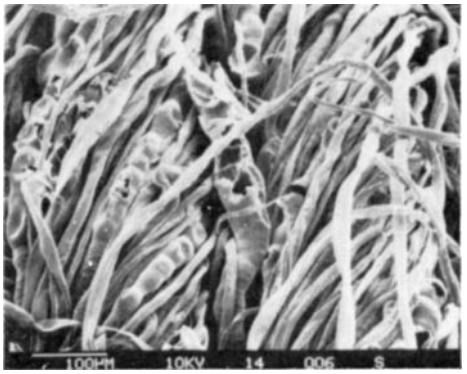


1 ⊢⊣ 200 μm

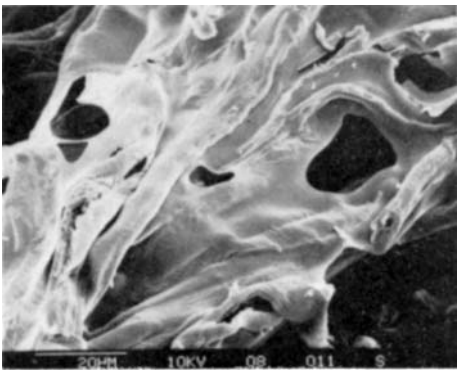


2 ⊢⊣ 10 μm

3a ⊢⊣ 50 μm

3b ⊢⊣ 20 μm

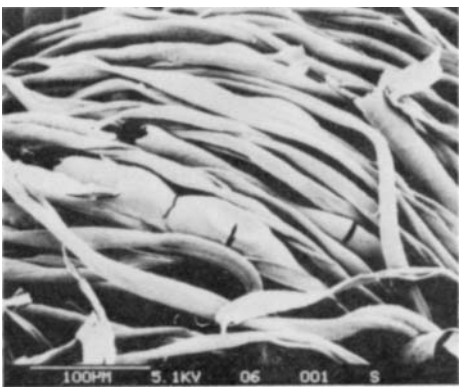


4 ⊢⊣ 50 μm

5a ⊢⊣ 50 μm

5b ⊢⊣ 50 μm

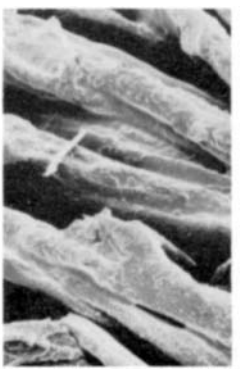

6a ⊢⊣ 20 μm

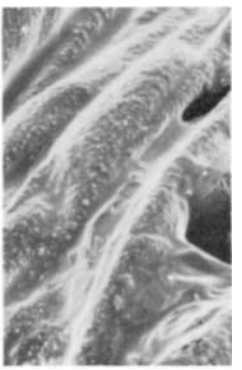

6b ⊢⊣ 10 μm

**Plate 25K — Fabrics after burning (continued).**
(1) Untreated cotton/wool fabric away from the charred region. (2) Melting of wool in hotter region. (3a,b), (4) Moving progressively closer to charred region of untreated cotton/polyester/wool fabric. (5a,b) Moderate and more severe damage to wool fibres in THPS-treated tri-blend fabric. (6) Charred region of (a) untreated and (b) treated tri-blend fabric.

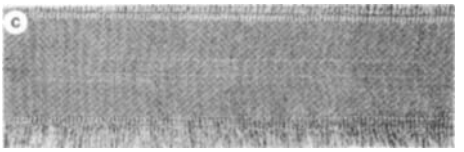

1

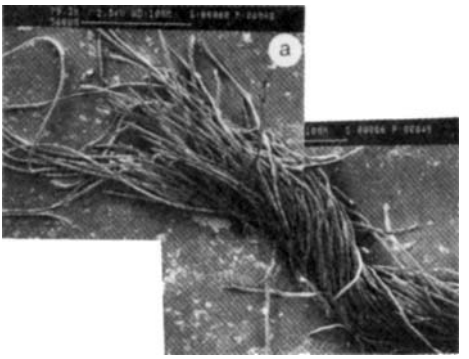

2

3

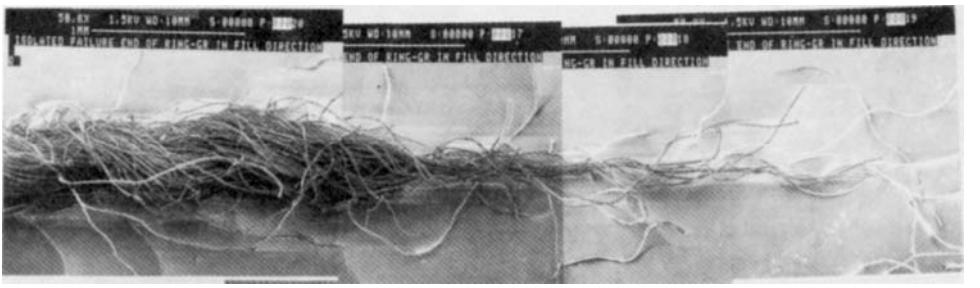

4

5

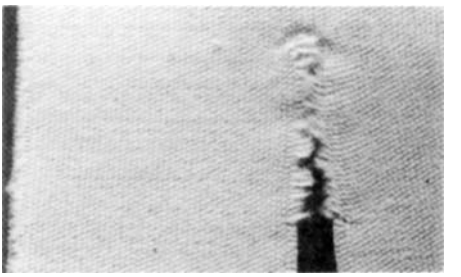

6

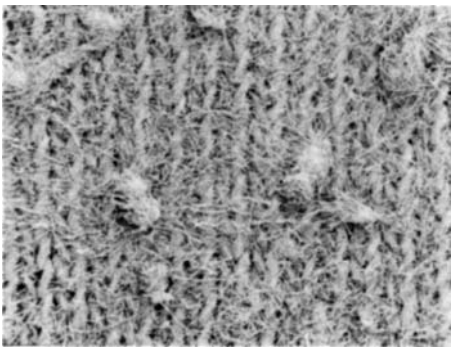

7

8

**Plate 25L — Break of yarns in woven fabric, Seo *et al* (1993).**
(1) Isolated failures in a ring-spun twill fabric. (2) Break of ring-spun cotton/polyester yarn in a twill fabric tensioned warpwise. (3) Detail of fibre breaks. (4) Break of similar yarn tensioned fillwise.
**Tongue tear of woven fabric, Scelzo *et al* (1994).**
(5) Loosely woven fabric. (6) Tighter fabric.
**Martindale abrasion of knit cotton.**
(7) Development of pills. (8) Break by multiple splitting.

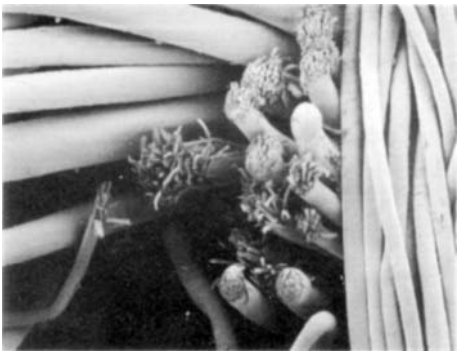

**1**

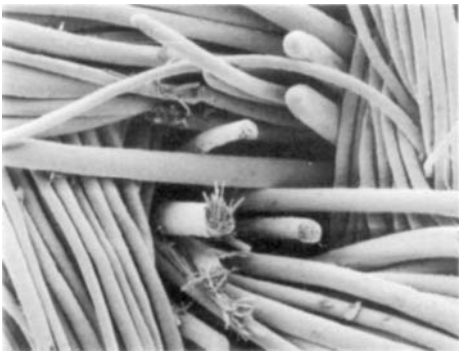

**2**

**3**

**4**

**5**

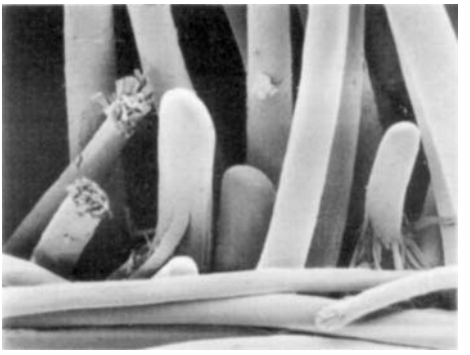

**6**

**Plate 25M — Abrasion of woven wool/mohair fabric.**
(1),(2) Wear at interstices between yarns. (3)–(6) Detail of fibre splitting and wear.

# 26

# COMPOSITE TESTING

Although most textile fabrics are used without any material added to the fibres, except for very thin layers of surface finish, there is an appreciable usage of fibres and fabrics in composite materials. This chapter gives some examples of failure testing in the composite form, both flexible and rigid. Some examples of failure in use of composites are included in Chapter 40.

As a means of evaluating the behaviour of flexible rubber/textile composites, as used for example in tyres, special laboratory specimens may be made up. For example, in order to test the effectiveness of adhesion between rubber and tyre-cord fabric, a thick sandwich is made with two fabric layers and three layers of rubber. The sandwich can then be torn apart, to give the form of surfaces indicated in Fig. 26.1, by the action shown in Fig. 26.2. A macrophotograph of the torn surfaces, **26A(1)**, shows that the failure is divided between different positions in the cross-section. In order to make identification easier, their locations are outlined in Fig. 26.1. Over the largest part of the surface. A, the separation is within the rubber, with occasional breaks through to the fabric on one side, B, or the other side, C. But there are clearly defined islands, where the separation is entirely between fabric and rubber, fabric side at D, rubber side at E. Naturally, the islands match on either side. The bare fabric surface appears lighter, and is lower than the surrounding area, A, while the mirror-image on the other side stands proud, and is identifiable by the regular lines of the replica of the yarns, which contrast with the more irregular tearing of the rubber in the surrounding region. Detail of failure at the fabric surface is shown in **28A(2)**. The fabric was a typical tyre-cord fabric with a strong warp of nylon, loosely held by a skeleton cotton weft. A typical cotton fibre tensile break is shown in **26A(3)**. The nylon fibres show either surface peeling, **26A(4)**, or a granular-type tensile break, **26A(5)**. The occurrence of a granular, rather than a ductile break is surprising: it might be due to some degradation or to the suppression of the usual crack propagation in the bonded composite.

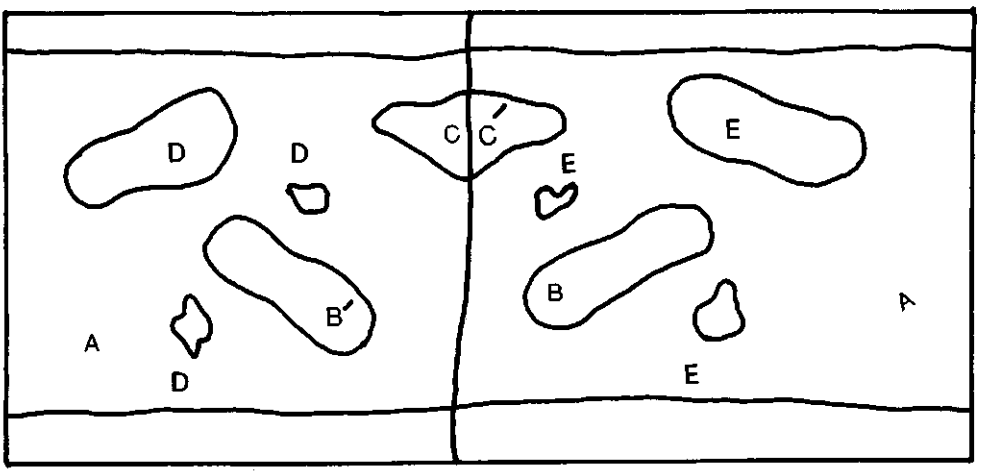


Fig. 26.1 — Identifications of regions in macrophotograph, **26A(1)**. Over most of the surface A failure is in the rubber, with occasional break-through to fabric. Failure is at the rubber–fabric interface in regions B and C, with the corresponding regions with fabric imprints at B′ and C′. Complete failure between rubber and fabric at positions D and E.

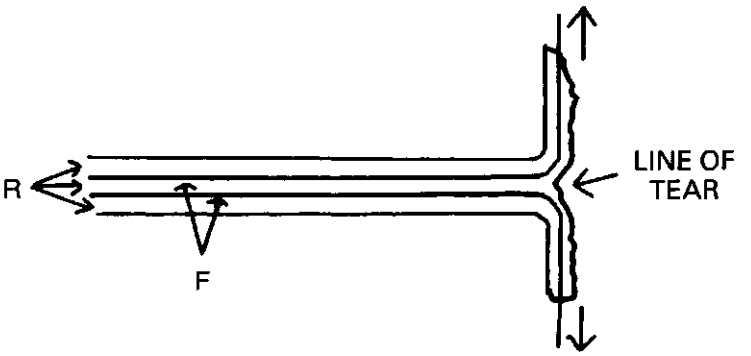


Fig. 26.2 — Tearing of test piece, with two layers of fabric F, sandwiched with three layers of rubber, R.

Another example is flex fatigue in a three-dimensional buckling mode of a thin rubber-coated fabric used in a metering device. It appears that failure starts with a loss of adhesion between rubber and fabric, and that the increased strain which this allows leads to rupture of the rubber layer, **26B(1)**. There may be some damage to fibres in the underlying fabric, **26B(2)**, but this is not a primary cause of failure.

Another test of a composite, PVC-coated polyester fabric used in flexible structures was designed to investigate chemical degradation. The investigation was carried out by Martin Ansell at the University of Bath and was briefly referred to in Chapter 16. In order to accelerate the degradation the material was boiled in water for several weeks and then broken in a tensile test. The control sample shows polyester fibre breaks with mushroom ends, **26B(3)**, typical of a high-speed break situation, probably resulting from transfer of load after break has started. After 3 weeks boiling, **26B(4)**, the breaks are mixed in form; but after 6 weeks, **26B(5)**, they are well-defined stake-and-socket breaks; after 8 weeks, **26B(6)**, embrittled rims become larger, and there are some changes in the appearance of the stake. These results were reported by Ansell (1983).

The study of fracture of rigid composites is a major subject in itself, and the forms of breakage depend on: (a) the type of fibre and matrix; (b) whether the composite structure has been made by dispersal of short fibres, by tape-laying of oriented pre-preg, by filament winding, by two-dimensional or three-dimensional textile structures, or by any other method; (c) the shape of the test specimen; (d) the form of loading. These larger-scale mechanical/geometrical aspects are beyond the scope of this book; and the account here is limited to some examples of failure at the level of fibre and matrix.

The main forms of failure have been categorized by Friedrich (1983) in a study of the fracture of a composite of short glass fibre in a polyethylene terephthalate matrix. A 'compact tension' specimen, illustrated in Fig. 26.3, was used. The fracture crack propagates from the tip of the preformed crack, AB, when the two arms are put under tension. This is termed mode I fracture, Fig. 26.4(a), because the crack opens under a tensile stress acting in a direction perpendicular to the plane of the crack.

Because the fibres are randomly arranged in all directions, the test shows examples of fracture both with the fibres lying across the crack and subject to a tensile stress along their length, and with the fibres lying in the crack plane so that the tensile stress is transverse to the

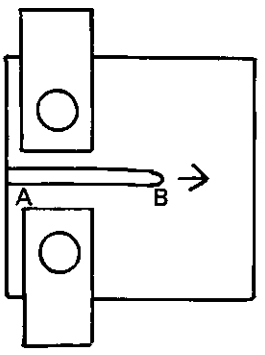


Fig. 26.3 — Compact tension test.

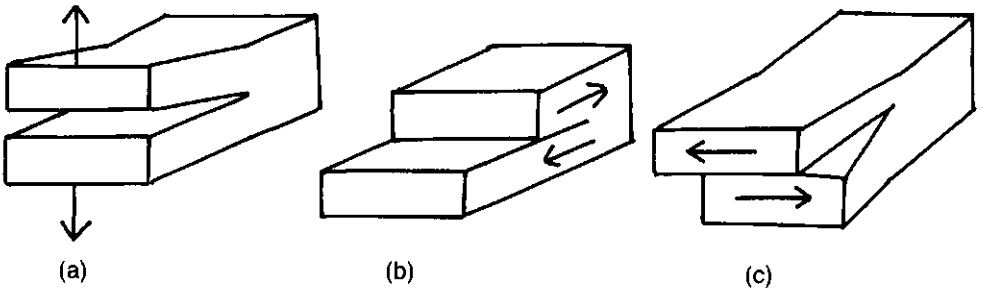


Fig. 26.4 — Forms of crack growth. (a) Mode I fracture under tensile stress perpendicular to the crack. (b) Mode II fracture under shear stress along the crack. (c) Mode III fracture under shear stress across the crack.

fibre axes and between fibres. In **26C(1)–(6)** and **26D(1),(2)**, the left-hand set shows SEM pictures taken in profile of the polished surface of a cut perpendicular to the plane of the crack, and the right-hand set shows the corresponding fracture surfaces.

The effects observed, and located on Fig. 26.5, are as follows:

(A) mechanical overload causing brittle fibre fracture, **26C(1),(2)**;
(B) fibre pull-out, without rupture, **26C(3),(4)**;
(C) delamination between fibre and matrix, **26C(5),(6)**;
(D) plastic deformation and rupture of the matrix, **26D(1),(2)**.

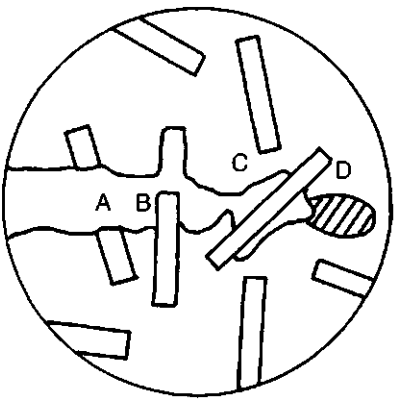


Fig. 26.5 — Mechanisms of failure at an advancing crack: (A) fibre fracture by overload; (B) fibre pull-out; (C) delamination; (D) matrix flow.

In addition, attack by a corrosive environment can lead to multiple fibre cracking, **26D(3),(4)**.

The effect of temperature on the fracture of the glass fibre/PET composite was also examined: the viscous flow of the matrix is much more pronounced at +60°C, **26D(5)**, than at −60°C, **26D(6)**.

Although the range of fibre orientations and local geometries causes different forms of failure to occur in the same short-fibre composite, larger-scale structural features do not appear in such a dispersed system. However, when yarns are regularly arranged in the composites, the structure shows up in the failure.

For example, both delamination and fibre breakage is found in the break of a cross-ply, $[90,0,90,0]_S$, laminate of carbon fibre in the form of continuous-filament yarn, with a matrix of nylon 12, applied as a powder and then thermally consolidated. Delamination in the plies containing filaments perpendicular to the tensile stress and fibre breakage in filaments lying parallel to the stress is shown in **26E(1)**.

If the reinforcement is a fabric the weave structure shows up at low magnification, as seen in **26E(2)** for a woven glass/polyamide composite. At higher magnification, **26E(3)**, the fibre fracture and delamination is more clearly shown. Similar effects were found in a woven carbon/epoxy composite, **26E(4)**.

More complex effects are shown with three-dimensional woven structures, illustrated here in work by Guenon (1987) on carbon fibre in epoxy. The test method used is a double cantilever beam with a pre-formed crack, but with Z-direction reinforcement it was necessary

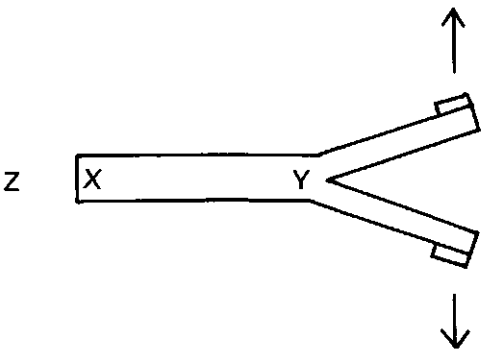


Fig. 26.6 — Double cantilever beam test (DCB).

to modify the usual test specimen, illustrated in Fig. 26.6, by sticking aluminium tabs on to the composite, in order to cause the crack to propagate along the specimen. There is then delamination for the two yarn layers parallel to the plane XY of the fabric, and rupture and pull-out of yarns in the Z-direction, **26E(5),(6)**.

The form of delamination is shown up in studies by Crick *et al.* (1987), of uniaxial APC-2 composites of carbon fibre in polyetheretherketone (PEEK) after crack propagation in a DCB test. At first there is a slow, stable crack growth, but this is followed by a fast, unstable fracture. Low-magnification views of fracture surfaces in the two regions are shown in **26F(1,2)**. More detail of the delamination is shown by cutting a cross-section through the crack in a fractured specimen embedded in an acrylic medium, polishing and then etching the surface, and finally dissolving away the acrylic in chloroform. In **26F(3),(4)**, the way in which the crack boundary follows a complicated profile within the matrix around the fibres can be seen. Particularly in the unstable region, there are large re-entrant cavities. There is a contrast between the considerable matrix flow in the stable region and the cleaner fracture in the unstable region, which is seen in more detail at the higher magnification, **26F(5),(6)**. The matrix surface shows evidence of spherulitic texture, and, especially in the stable region, of cracks or crazes, shown up by the etching, parallel to the fracture surface.

The glass and carbon fibres in the rigid composites illustrated in **26C-F** have roughly equal strength in all directions and break with sharp brittle fractures. A different situation exists with highly oriented linear polymer fibres, which easily split axially and fibrillate, as demonstrated by the work of Matsuda (1987) on composites of the aramid copolymer fibre Technora with an epoxy matrix. In a DCB test on a uniaxial laminate, there is substantial fibre and fibril bridging across the crack, **26G(1)**. Detail of the fibrillation, together with some delamination, is shown in **26G(2)**.

In addition to examining the mode I fracture, shown in Fig. 26.4(a), with the tensile stress opening the crack, Matsuda also used an end-notch flexure (ENF) specimen to study mode II fracture. In this test method, shown in Fig. 26.7, change in curvature generates the shear stress along the crack, Fig. 26.4(b), and causes the crack to grow. An overall low-magnification view of the fractured sample, **26G(3)**, shows the Teflon film separator, a mode I pre-crack, then the mode II fracture starting in stable growth, and beyond a critical crack depth becoming unstable. In the stable region there is extensive fibrillation, **26G(4)**, but in the unstable region there is matrix flow and delamination, **26G(5)**.

Matsuda also examined Technora/epoxy composites in compression, and the failed specimens show the large-scale kinking, which occurs in a uniaxial composite compressed in the orientation direction, **26G(6)**, and the delamination and slip in the 90° test, **26G(7)**.

Mode II fracture by the ENF test has also been studied by Trethewey (1986), for carbon fibre composites, and the SEM pictures show up the difference between the mode I pre-crack and the mode II fracture surface for AS4 carbon fibre in epoxy, **26H(1),(2)**, and APC-2 carbon fibre in the thermoplastic PEEK, **26H(4),(5)**. The appearance is somewhat different in mode II fatigue fractures, **26H(3),(6)**.

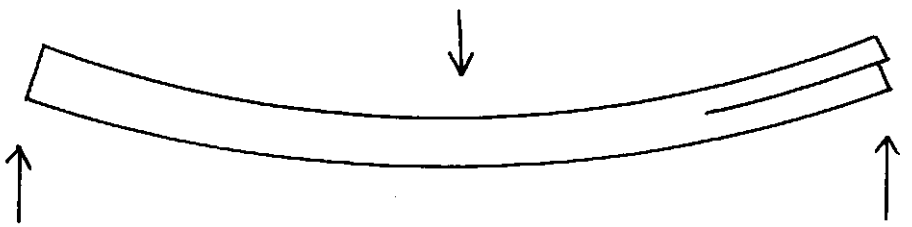

Fig. 26.7 — End-notch flexure test (ENF).

It has been found by Becht (1988) that the appearance of mode III fracture in carbon fibre/epoxy laminates is similar to mode II.

In test situations where fibres break, the simple and characteristic forms of fracture within composites are seen as brittle fracture in glass fibres, **26H(7a,b),** from Valentin, Paray and Guetta (1987), and as granular fracture in carbon fibres, **26H(8),** from Beaumont (private communication).

However, under some types of stress, there can be an axial splitting of carbon fibres. This implies that the transverse strength of the fibre is less than that of the fibre/matrix interface, and occurs with pitch-based carbon fibres. An example of crack propagation, partly across and partly around the carbon fibres, is shown in **26I(1),** which is a polished section which has been subject to severe thermal shock. The characteristic structure of pitch-based fibres, illustrated in Fig. 26.8, can be seen in **26I(2),** in which the fibres have broken over a transverse cross-section. Some delamination can also be seen. It is this layered form, which leads to the axial splitting shown in **26I(3),(4)**, as a result of transverse tension. If the layers are perpendicular to the tension, there is splitting, but, if they are in line with the tension, there is none. Axial splitting of fibres has also been seen in pitch-based fibre/epoxy composites.

There are differences between different types of pitch-based fibre, as seen in **26I(5),** which shows a different texture of failure surface from **26I(2)**. In a PAN-based fibre composite, illustrated in **26I(6),** thermal shock causes cracking with delamination but no fibre splitting.

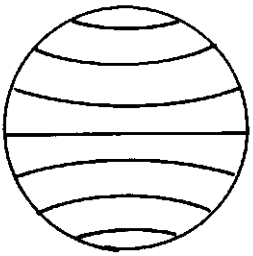

Fig. 26.8 — Characteristic structure of pitch-based carbon fibres.

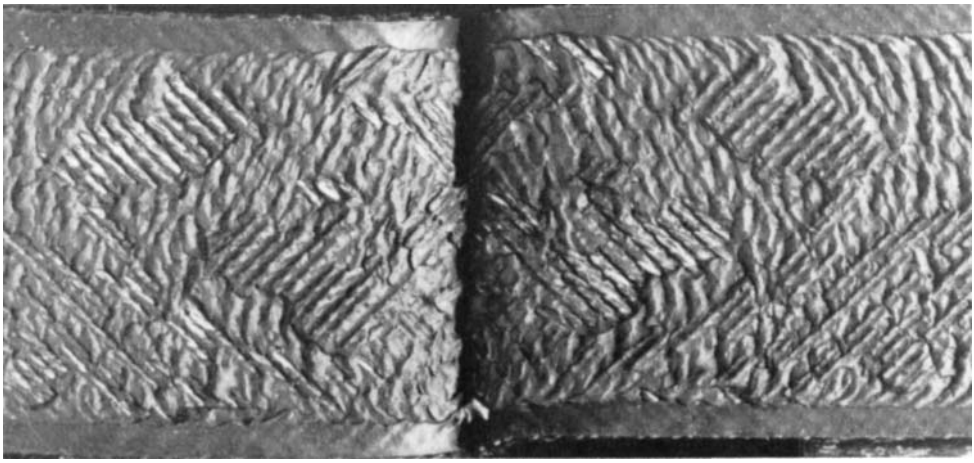

1

2 ⊢—⊣ 100 μm

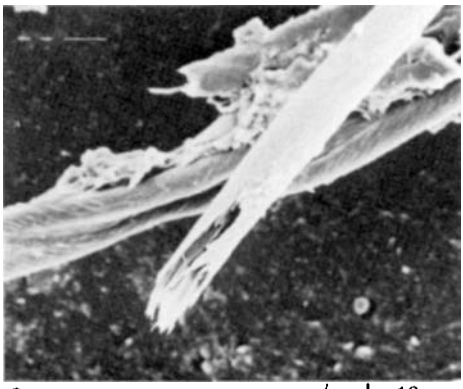

3 ⊢—⊣ 10 μm

4 ⊢—⊣ 10 μm

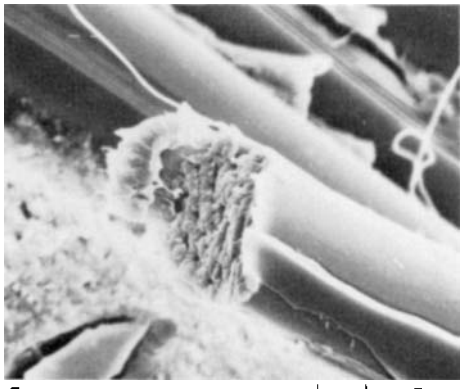

5 ⊢—⊣ 5 μm

**Plate 26A — Testing of fibre/rubber bonding by pulling apart a double sandwich of fabric in rubber.** (1) Macrophotograph of torn surfaces. See Fig. 26.1 for identification of regions of failure. (2) From failure zone between rubber and fabric. (3)–(5) Detail of damage to fibres.

1 20 $\mu$m

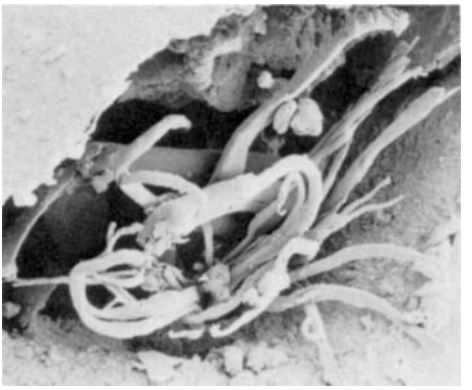

2 1 mm

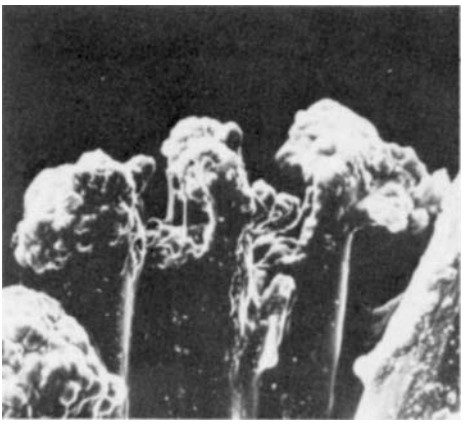

3

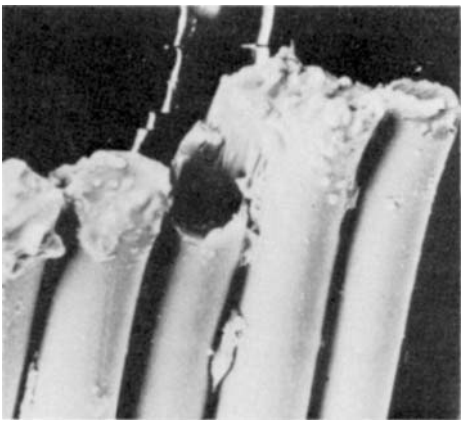

4

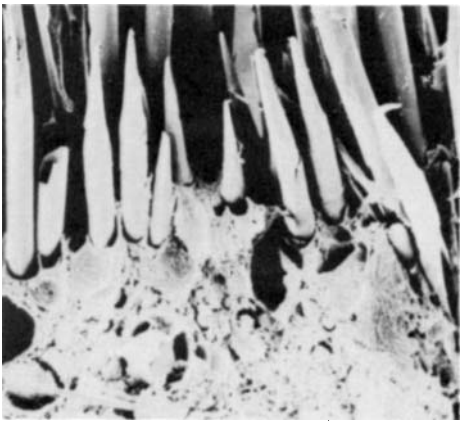

5

6

**Plate 26B — Three-dimensional buckling fatigue of thin rubber-coated fabric.**
(1) Initial appearance of damage. (2) Detail of fabric.
**Accelerated degradation of polyester fabric coated with a 1mm layer of pigmented and stabilized plasticized PVC; fabric weight was 280 g/m$^2$ and coating was 600 g/m$^2$; boiled in distilled water (100°C); then subjected to a tensile test. SEM pictures by courtesy of Martin Ansell, University of Bath.**
(3) Control sample, not boiled. (4) After 3 weeks boiling. (5) After 6 weeks boiling. (6) After 8 weeks boiling.

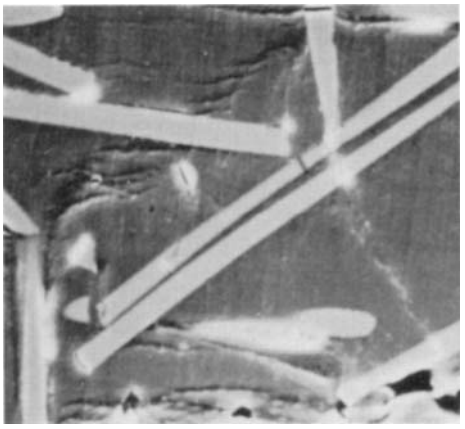

1

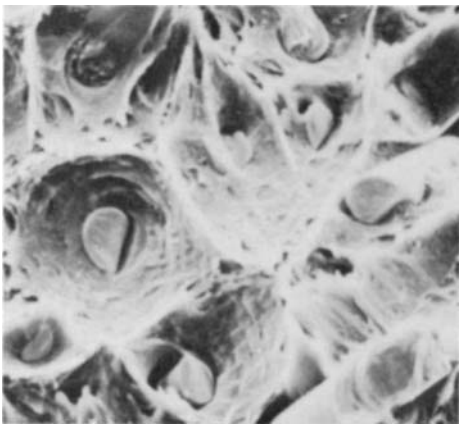

2

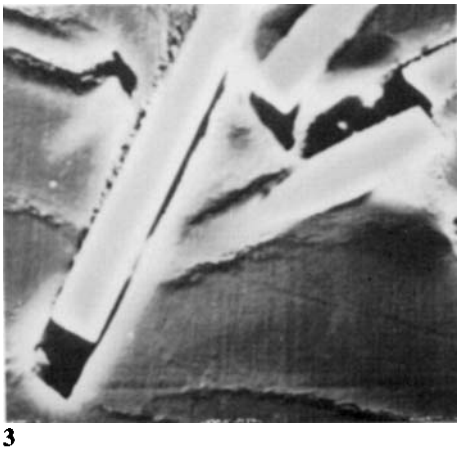

3

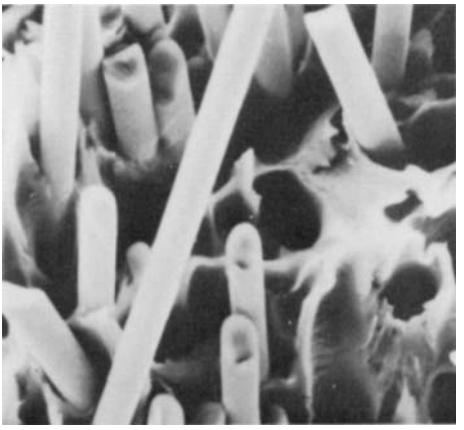

4

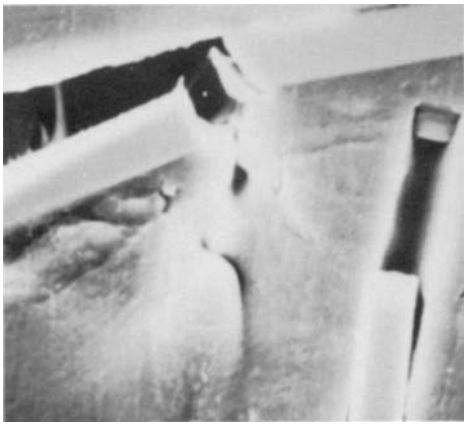

5

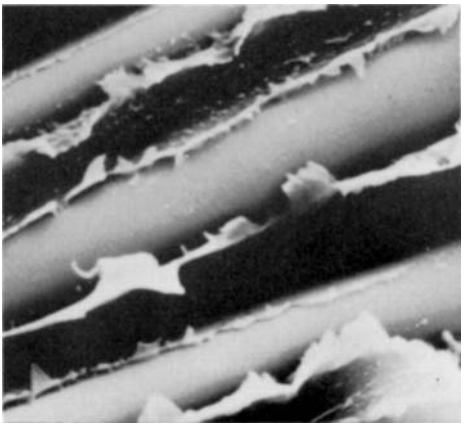

6

**Plate 26C — Tensile fracture at an advancing crack tip in a compact tension specimen of a short glass fibre/PET composite (from K. Friedrich, 1983).**

Note: Left-hand set (odd numbers) are polished surface profiles and right-hand set (even numbers) are fracture surfaces. Locations, A to D, are shown in Fig. 26.5. (1),(2) Fibre fracture by mechanical overload, A. (3),(4) Fibre pull-out, B. (5),(6) Delamination, C.

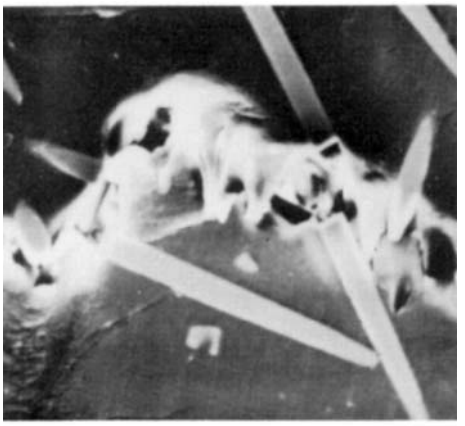

1

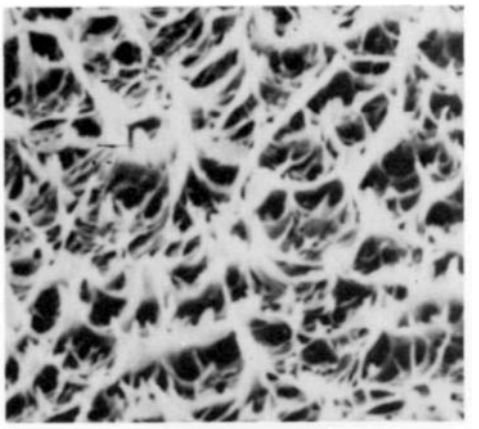

2

3

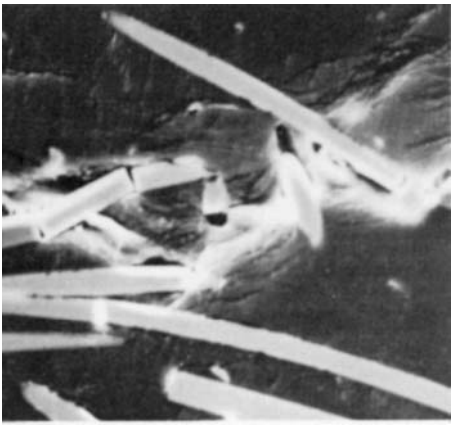

4

5 50 $\mu$m

6 50 $\mu$m

**Plate 26D — Fracture at crack tip in glass fibre/PET composite (continued).**
(1),(2) Plastic deformation of matrix, D. (3),(4) Multiple fibre cracking due to an additional corrosive environment. (5) Fracture surface, tested at +60°C. (6) Fracture surface, tested at −60°C.

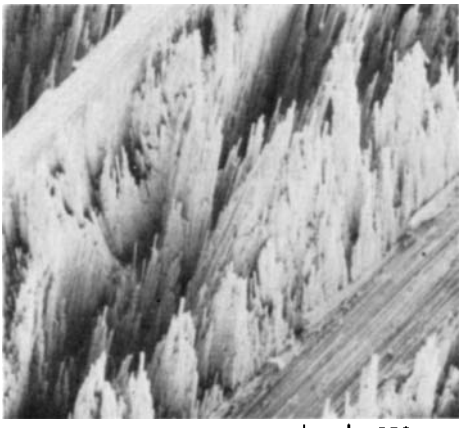

1 200 μm

2 200 μm

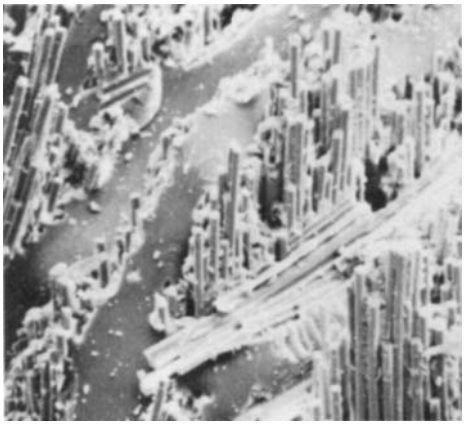

3 50 μm

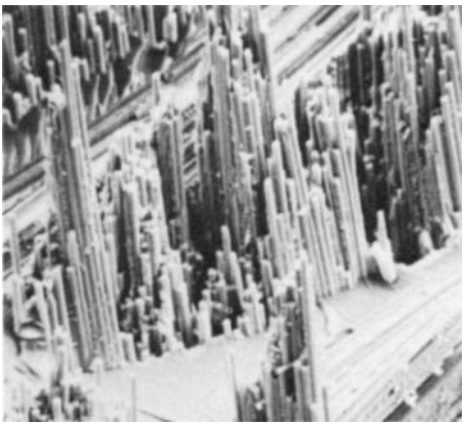

4 50 μm

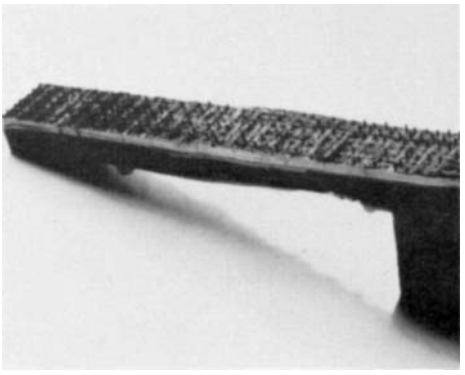

5

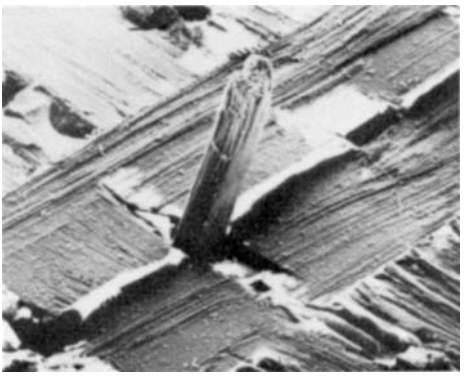

6

**Plate 26E — Effects in structured composites (from K. Friedrich, 1983).**
(1) Cross-ply carbon fibre/nylon 12 composite. (2),(3) Woven glass (continuous filament) fabric in polyamide. (4) Woven carbon (continuous filament) in epoxy.
**Fracture of a three-dimensional woven carbon/epoxy composite with crack propagation in a DCB specimen (from V. A. F. Guenon, 1987).**
(5) Photograph of failure. (6) SEM view of detail, with X and Y directions running along diagonals, and a Z direction yarn projecting.

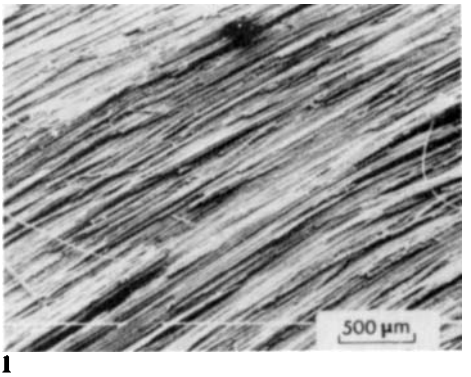

1

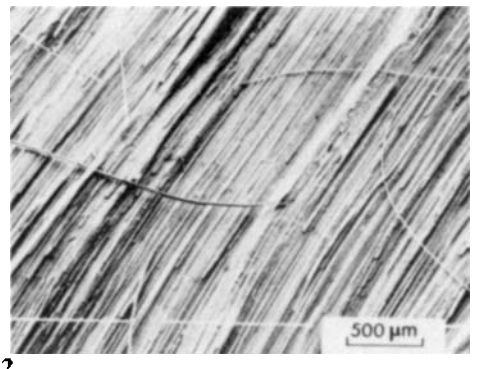

2

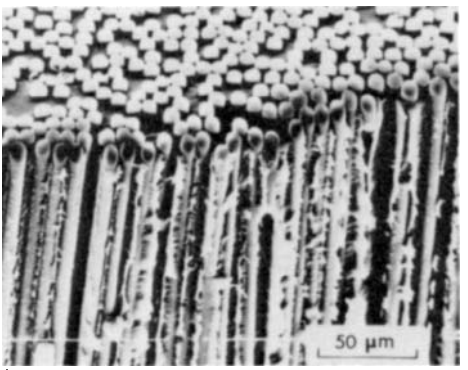

3

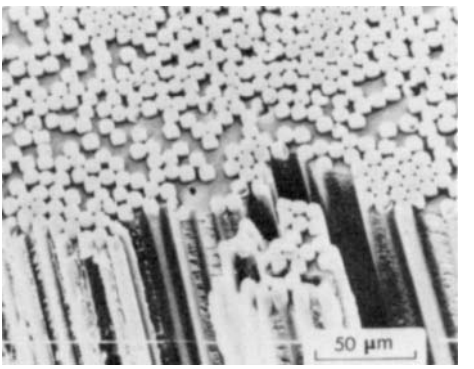

4

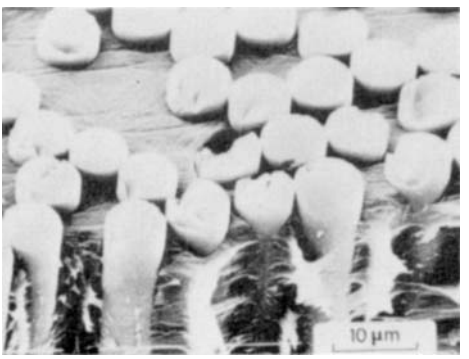

5

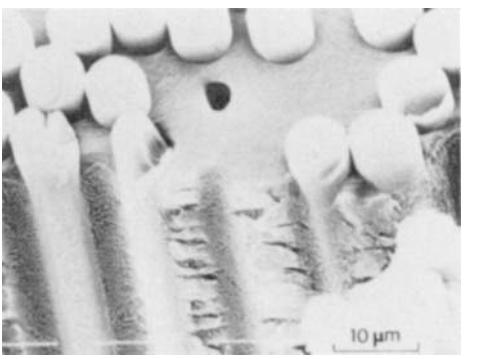

6

**Plate 26F — Fracture of carbon fibre/PEEK composites in DCB test (from Crick *et al*, 1987).**
(1) Stable crack growth region. (2) Unstable crack growth region.
**Intersection of polished and etched cross-sectional surface with fracture surface.**
(3),(5) Stable crack growth region. (4),(6) Unstable crack growth region.

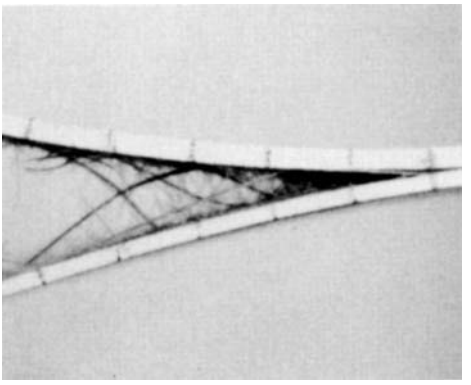

1

2

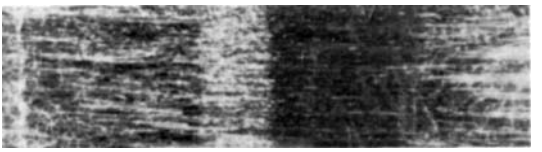

4

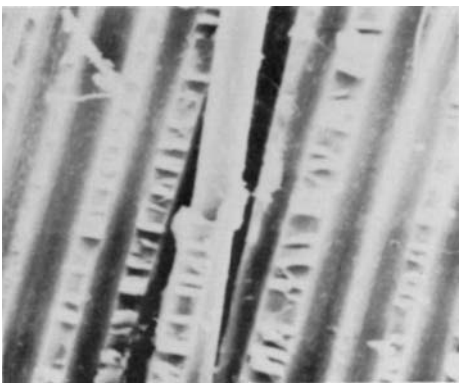

5

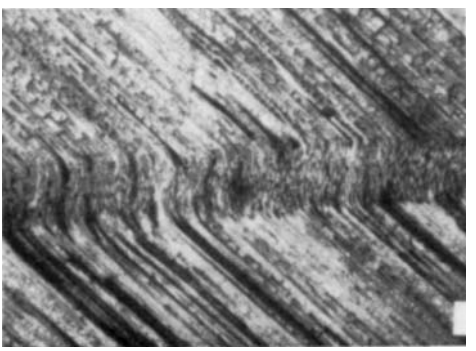

6

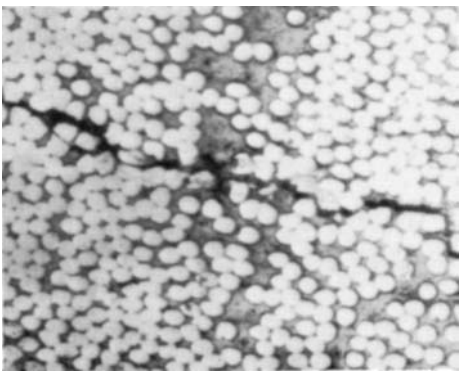

7

**Plate 26G — Fracture of uniaxial Technora/epoxy composites (from T. Matsuda, 1987).**
(1),(2) DCB test, mode I fracture. (3) ENF-fractured specimen showing, from left to right (a) Teflon film, (b) mode I precrack, (c) stable mode II crack growth, (d) unstable mode II failure. (4) Stable mode II fracture. (5) Unstable mode II fracture. (6) Compression failure in 0° test. (7) Compression failure in 90° test.

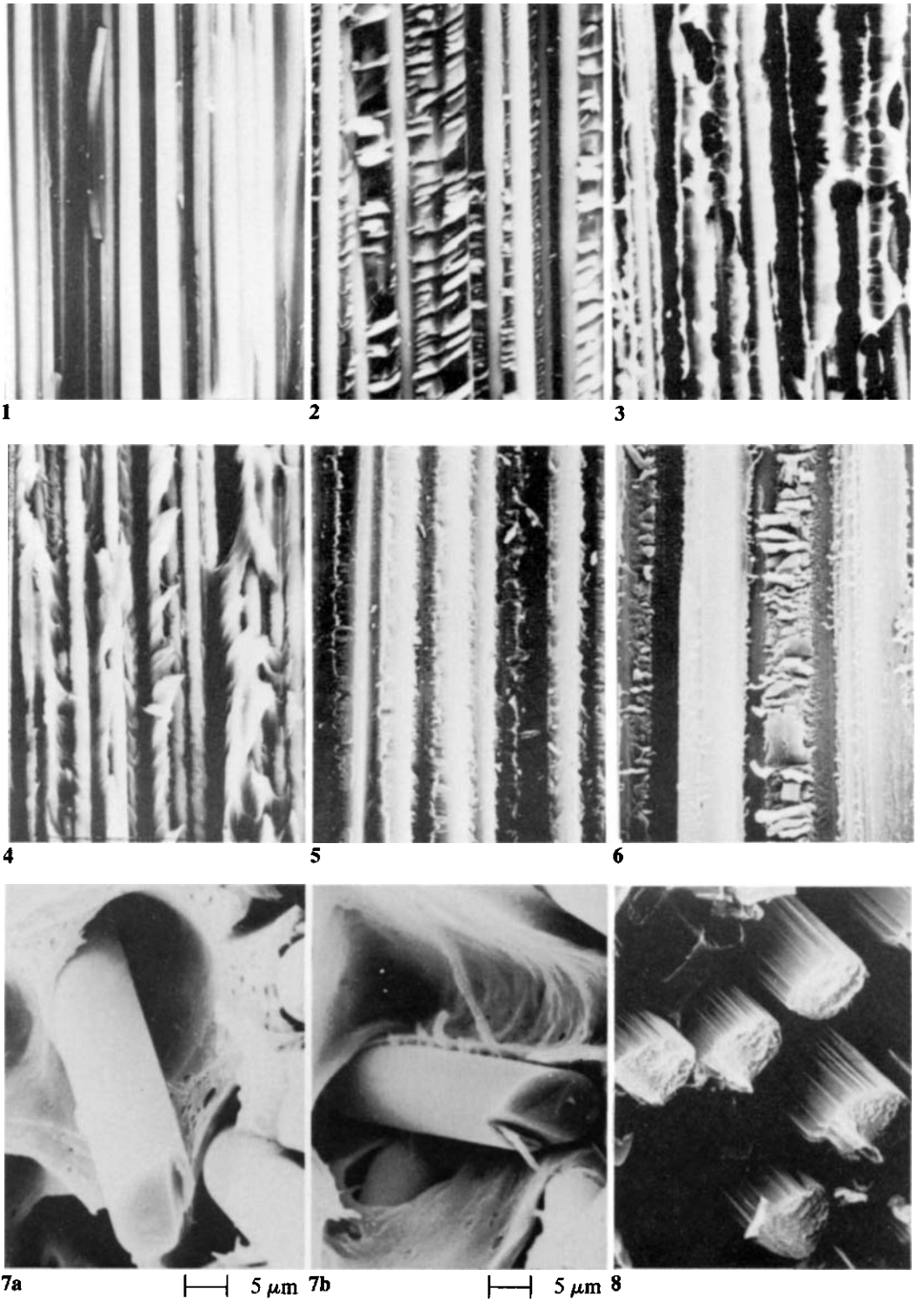


**Plate 26H — Fracture of carbon fibre composites (from B. R. Trethewey, 1986).**
(1) ENF test of AS4/epoxy, mode I pre-crack. (2) ENF test of AS4/epoxy, mode II. (3) Mode II fatigue test of AS4/epoxy. (4) ENF test of APC-2/PEEK, mode I pre-crack. (5) ENF test of APC-2/PEEK, mode II. (6) Mode II fatigue test of APC-2/PEEK.
**Bending failure of glass fibre/nylon 66 composite (from Valentin, Paray and Guetta 1987).**
(7a,b) Brittle fracture of glass fibres.
**Torsion failure in carbon fibre/polyester resin composite with poor bonding (from P. W. R. Beaumont, private communication).**
(8) Granular fracture of carbon fibres.

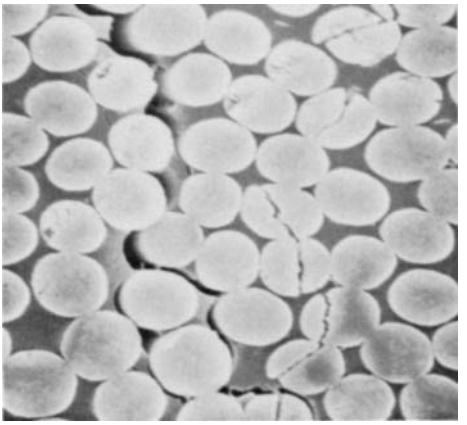

1 10 μm

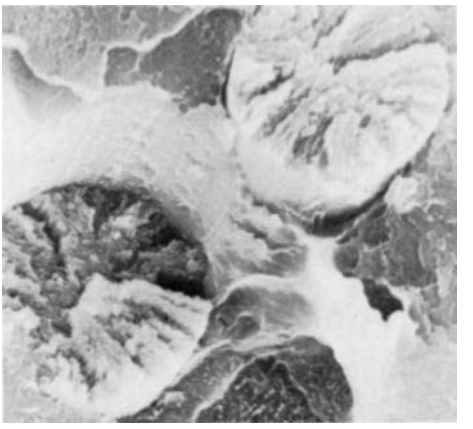

2 2 μm

3 5 μm

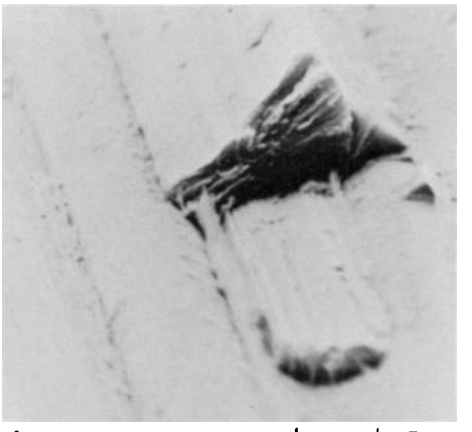

4 5 μm

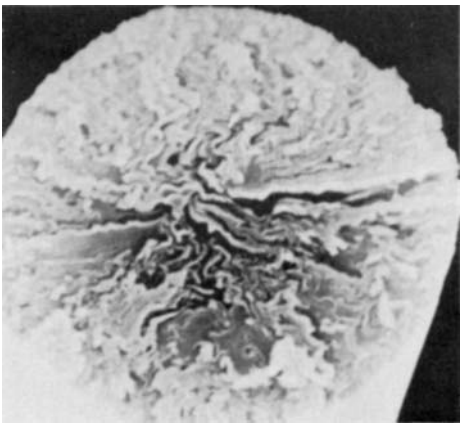

5 1 μm

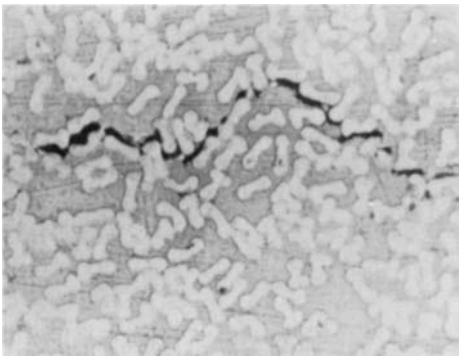

6

**Plate 261 — Fractures in experimental Thornel P75 pitch-based carbon fibre/PEEK composites (from Barnes, private communication).**
(1) Polished section of ±30° composite, cycled ten times in and out of liquid nitrogen. (2) Unidirectional composite, failed in longitudinal flexure. (3),(4) Unidirectional composite failed under transverse tension in a cantilever beam test.
**Fractures in other experimental carbon fibre/PEEK composites (from Barnes, private communication).**
(5) Nippon XN 50 pitch-based fibre in unidirectional composite, failed in longitudinal flexure. (6) Optical micrograph of polished section of Hoechst/Celanese GY70 PAN-based fibre in 0/90 composite, after cooling to room temperature.